# *Arabidopsis* inositol polyphosphate kinases regulate COP9 signalosome functions in phosphate-homeostasis

Yashika Walia[1], Kishor D Ingole[1,2], Mritunjay Kasera[1], Swaroop Peddiraju[1], Debabrata Laha[3], Gabriel Schaaf[4], and Saikat Bhattacharjee[1*]

[1]Laboratory of Signal Transduction and Plant Resistance, UNESCO-Regional Centre for Biotechnology (RCB), NCR Biotech Science Cluster, 3rd Milestone, Faridabad-Gurgaon Expressway, Faridabad- 121 001, Haryana, India.

[2]Kalinga Institute of Industrial Technology (KIIT) University, Bhubaneswar- 751 024, Odisha, India.

[3]Department of Biochemistry, Indian Institute of Science, Bengaluru, Karnataka- 560 012, India.

[4]Department of Plant Nutrition, Institute of Crop Science and Resource Conservation, Rheinische Friedrich-Wilhelms-Universität Bonn, 53115 Bonn, Germany.

*Corresponding author:

Saikat Bhattacharjee

saikat@rcb.res.in

Tel: (+91) 0129-2848837

**ORCID ID**

Saikat Bhattacharjee https://orcid.org/0000-0003-1369-7700

Gabriel Schaaf https://orcid.org/0000-0001-9022-4515

Yashika Walia https://orcid.org/0000-0001-8122-8661

Kishor D Ingole https://orcid.org/0000-0003-1946-6639

Mritunjay Kasera https://orcid.org/0000-0002-1110-3502

Swaroop Peddiraju https://orcid.org/0000-0001-5290-7067

Debabrata Laha https://orcid.org/0000-0002-7823-5489

**Abstract**

**Targeted protein degradation is essential for physiological development and adaptation to stress. Mammalian INOSITOL PENTAKISPHOSPHATE KINASE (IP5K) and INOSITOL HEXAKISPHOSPHATE KINASE 1 (IP6K1) pair modulates functions of Cullin RING Ubiquitin E3 ligases (CRLs) that execute targeted degradation of substrates. Coordinated activities of these kinases protect CRLs on a COP9 signalosome (CSN) platform and stimulates deneddylation-dependent disassembly to maintain continuity of its functions. In plants, CRL regulations on CSN by inositol phosphate (InsP) kinases are not known. Here, we show interactions of *Arabidopsis thaliana* INOSITOL PENTAKISPHOSPHATE 2-KINASE 1 (IPK1) and INOSITOL 1,3,4-TRISPHOSPHATE 5/6-KINASE 1 (ITPK1), counterparts of the above InsP-kinase pair, with CSN subunits and its positive influences on the dynamics of cullin deneddylation. We identify neddylation enhancements on CRLs as an early response to phosphate-starvation and its orchestration by perturbed IPK1/ITPK1 activities. At a molecular level, specific kinetics of CSN5 deneddylase is affected by the above InsP-kinases. Overall, our data reveal conserved InsP-kinase involvements on CRL-CSN synergism in plants.**

61 **Introduction:**

62 The versatile functions of inositol phosphates (InsPs) in multiple cellular processes of all
63 eukaryotes is owed to its propensity for differential degree of phosphorylation catalyzed by
64 relatively conserved set of InsP-kinases[1-4]. In plants, $InsP_6$ (myo-inositol-1,2,3,4,5,6-
65 hexakisphosphate or phytic acid), produced by INOSITOL PENTAKISPHSPHATE 2-
66 KINASE 1 (IPK1) is sequentially (pyro)-phosphorylated by INOSITOL 1,3,4-
67 TRISPHOSPHATE 5/6-KINASES (ITPK1/2) and then by DIPHOSPHOINOSITOL
68 PENTAKISPHOSPHATE KINASES (PPIP5K or VIH1/2) to generate energy-rich
69 phosphoanhydride bond-containing inositol pyrophosophates (InsPP) $InsP_7$ and $InsP_8$,
70 respectively[5-8]. While $InsP_6$ or more recently speculated $InsP_7$, promotes auxin-dependent
71 degradation of AUX/IAA repressors, $InsP_8$ targets JASMONATE ZIM-DOMAIN (JAZ)
72 repressors[7,9-11]. Reduced $InsP_8$ levels during phosphate (Pi)-deprivation liberates the
73 transcription factor PHOSPHATE STARVATION RESPONSE 1 (PHR1)[12] to cause activation
74 of phosphate-starvation inducible (PSI) genes, but also subsequently targets its captor SPX1
75 (SYG1/Pho81/XPR1-domain containing protein1) for 26S proteasome-mediated
76 degradation[13-17]. Taken together, roles of InsP(P)s clearly include biochemical regulators of
77 stimulus-dependent substrate stabilities.

78 In a typical eukaryotic cell, ~20% of targeted protein degradation are mediated by Cullin RING
79 E3 ubiquitin ligases (CRLs)[18,19] that require covalent modification of a Nedd8 moiety on cullins
80 (CULs) (a process termed as neddylation)[19]. In absence of cognate substrates self-
81 ubiquitinylation-vulnerable CRLs are protected on Constitutive photomorphogenesis 9
82 signalosome (CSN), an evolutionarily conserved eight-subunit (CSN1-8) macromolecular
83 complex[20,21]. The CSN5 subunit in this complex contains an MPN+/JAMM metalloprotease
84 motif that catalytically removes Nedd8 (deneddylation) from CULs[22] causing CRL
85 disassembly and promoting newer associations required for continuum of its functions.

86 Optimal CRL activity hence necessitates regulated neddylation/deneddylation cycles of CULs.
87 Apparent contradiction between genetic requirements of the CSN-protection versus its
88 deneddylation activity on CRLs forms the basis of the 'CSN paradox'[23]. In mammals, locale-
89 specific coordinated activities of IP5K with IP6K1, functional homologs of Arabidopsis IPK1
90 and ITPK1, respectively provide $InsP_6$ to strengthen or $InsP_7$ to loosen CRL-CSN
91 associations[24-26]. Interaction changes affect cellular ratio of neddylated CUL: unneddylated
92 CUL ($CUL^{Nedd8}$:CUL)[26]. Here we show that Arabidopsis IPK1-ITPK1 pair retains conserved
93 CSN interactions and modulate CSN5 deneddylase dynamics. Pi-deprivation is perceived early
94 at CSN, and causes a shift in equilibrium of CRL deneddylation cycle via a response that
95 precedes PHR1-mediated transcriptional changes. Inhibitions of IPK1, ITPK1 or CSN5
96 activities result in constitutive phosphate-starvation response (PSR) even under sufficient Pi
97 availability. However, when actually Pi-starved, PSR responses are suppressed in these plants.
98 Our investigations reveal linked activities of IPK1-ITPK1 pair on CRL-CSN regulations of Pi-
99 homeostasis in plants.

100

101 **Results**

102 **Arabidopsis IPK1 and ITPK1 interact with CSN holo-complex.** Mammalian IP5K co-
103 precipitates with CSN2/5 whereas IP6K1 interacts with CSN1/2[25,26]. Arabidopsis ITPK1 has
104 been previously reported to associate with CSN1[27]. Interactions of Arabidopsis IPK1 with CSN
105 subunits have not been investigated earlier. We immuno-enriched Myc-IPK1 or ITPK1-GFP
106 from *ipk1-1*:*Myc-IPK1* and *itpk1-2*:*ITPK1-GFP* transgenic lines, respectively and probed for
107 the presence of selective CSN subunits, CUL1 or the substrate adaptor ASK1. These transgenic
108 lines restore high endogenous Pi and elevated PSI-gene *SPX1* expressions to wild-type (Col-0)
109 levels implicating the functionality of the corresponding fusion proteins[9] (Extended Data Fig.

110 1). In immunoprecipitation assays, CSN1/2/4/5, CUL1 and ASK1 co-purified with IPK1,
111 whereas ITPK1 enrichments detected CUL1, ASK1, and CSN1/2 but not CSN4/5 subunits
112 (Fig. 1a-b). This matches mammalian ITPK1 interactions with CSN1 but not CSN5[28]. Through
113 Biomolecular Fluorescence Complementation (BiFC) assays IPK1 or ITPK1 association with
114 CSN1 and CSN2 are detected as nucleocytoplasmic complexes similar to localization of the
115 individual proteins[6] (Fig. 1c-d; Extended Data Fig. 2). A negative control β-Glucuronidase
116 (GUS) protein does not interact with IPK1, ITPK1 or CSN1/2 (Extended Data Fig. 2). These
117 data suggest that likewise to animals, CSN associations of IPK1 and ITPK1 are conserved in
118 Arabidopsis. Although biochemically coupled through substrate-product relationship,
119 interaction between IPK1 and ITPK1 has not been demonstrated *in planta*. To this end, we
120 performed co-immunoprecipitation assays via transient co-expression of Myc-IPK1 and GFP-
121 ITPK1. Enrichment of GFP-ITPK1 with anti-GFP affinity beads co-elutes Myc-IPK1
122 indicating their associations *in vivo* (Fig. 1e). As earlier, via BiFC IPK1-ITPK1 complexes are
123 detected at nucleocytoplasmic locales (Extended Data Fig. 2). Interaction assays *in vitro* with
124 recombinant His-IPK1 and GST-ITPK1 further confirm direct association between these
125 proteins (Fig. 1f). Overall, our results recapitulate IPK1 and ITPK1 interactions with CSN and
126 with each other.

127 To determine the cellular proportions of IPK1 or ITPK1 that associate with or are independent
128 of the CSN holo-complex, we subjected Col-0, *ipk1-1*:*Myc-IPK1* and *itpk1-2*:*ITPK1-GFP*
129 extracts to size-exclusion chromatography followed by immunoblots for detecting
130 representative CSN subunits, Myc-IPK1 or ITPK1-GFP. The elution patterns of molecular
131 weight standards and selective CSN subunits with demarcation of CSN holo-complex fractions,
132 as noted in several earlier reports are shown[29,30] (Fig. 2a). CSN1, exclusively associates with
133 the CSN holo-complex and elutes accordingly in higher molecular weight pools (400-600 kDa).
134 CSN5 fractionates both as a part of CSN holo-complex as well as in lower molecular weight

135 pools (monomers, 100-50 kDa). Partitioning profiles of CSN5 and CSN4 are comparable
136 between Col-0, *ipk1-1*:*Myc-IPK1* and *itpk1-2*:*ITPK1-GFP* (Fig. 2c; Extended Data 3).
137 Remarkably, neither Myc-IPK1 nor ITPK1-GFP proteins are detected in fractions
138 corresponding to the CSN holo-complex implying that these associations are either transient
139 or represent only a marginal proportion of these proteins (Fig. 2a). Co-elution of Myc-IPK1
140 and ITPK1-GFP in overlapping fractions is likely indicative of their *in vivo* associations we
141 noted earlier.

142 **CSN5 deneddylase deficiencies of CSN cause enhanced CUL1 neddylation in *ipk1* or *itpk1***
143 **mutant.** Depletion of IP5K or IP6K1 reduces CRL-CSN associations in mammalian
144 systems[24,25]. To examine whether in *ipk1-1* or *itpk1-2* lower CUL1 pools co-fractionate with
145 the CSN holo-complex, extracts from these plants and Col-0 were fractionated as earlier and
146 compared for elution profiles of CSN subunits and CUL1. Although CSN1/4 or CUL1 profiles
147 are comparable (Fig. 2a-b; Extended Data 3), increased CSN5 presence in fractions
148 corresponding to CSN holo-complex with a concomitant decrease in the monomeric elutions
149 is apparent for *ipk1-1* or *itpk1-2* when compared to Col-0 (Fig. 2c). Total levels of CSN5
150 however are unaffected in these mutants. Taking into account that overall CUL1 profiles are
151 comparable, CRL assemblies or CRL-CSN associations are likely not perturbed in the *ipk1-1*
152 or *itpk1-2* plants. Immuno-enrichments of CUL1 although is slightly lower from *ipk1-1* or
153 *itpk1-2* than Col-0, nonetheless proportionately similar amounts of CSN1/2 as in Col-0 are
154 bound to it further supporting the above conclusion (Extended Data Fig. 4).

155 Resident CSN5 performs the deneddylase role in a CSN holo-complex[22]. This raised the
156 intriguing possibility whether changed partitioning of CSN5 in *ipk1-1* or *itpk1-2* impact CSN-
157 mediated deneddylation efficiencies on CRLs. Indeed, as a consequence of depleting IP5K or
158 IP6K1 in mammalian system steady-state ratio of $CUL1^{Nedd8}$:CUL1 are perturbed to cause
159 strong increments in $CUL^{Nedd8}$ levels[25,26]. Remarkably, in *ipk1-1* or *itpk1-2* lysates, enhanced

160 CUL1$^{Nedd8}$ levels relative to Col-0 are strikingly prominent (Fig. 2d). Extracts from *ipk2β-1*
161 with low $InsP_6$ levels as *ipk1-1*[2], or *vih2-4* plants with elevated $InsP_7$ [7] does not show elevated
162 CUL1$^{Nedd8}$ pools as in *ipk1-1* or *itpk1-2* (Extended Data Fig. 5). A modest decrease in
163 CUL1$^{Nedd8}$:CUL1 ratio is however consistently noted in *ipk2β-1*. In the respective
164 complemented lines of *ipk1-1* or *itpk1-2*, CUL$^{Nedd8}$:CUL ratios are restored comparable to Col-
165 0 (Fig. 2d).

166 Global ubiquitinylation is enhanced due to loss of mammalian IP6K1[25]. As a possible
167 consequence to increased CUL$^{Nedd8}$ levels, we tested relative levels of ubiquitinylation in Col-
168 0, *ipk1-1*, or *itpk1-2* extracts. Clear increase in global ubiquitin-conjugates in appearance of a
169 smear when probed with anti-ubiquitin antibodies is detected in the mutant plants than Col-0
170 (Fig. 2e). In complemented lines, wild-type ubiquitinylation levels are noted. Further, in-lysate
171 deneddylation assay to determine deneddylase defects[24] reveal decreased efficiencies of CUL1-
172 deneddylation by endogenous CSN5 simultaneous with increased CUL1 turnover rates in *ipk1-*
173 *1* or *itpk1-2* extracts (Fig. 2f). This decrease in stability likely accounts for the reduced
174 immuno-enrichments from the mutants observed earlier. Taken together, our results parallel
175 animal studies and point to impaired CSN-deneddylation activity in *ipk1-1* or *itpk1-2*, that lead
176 to augmented CUL1$^{Nedd8}$:CUL1 ratios with increased CUL1 turnover due to self-
177 ubiquitinylation.

178 **Down-regulation of CSN deneddylase activity resulting in increased CUL1 neddylation**
179 **occur during PSR.** Common consequences in *ipk1-1* and *itpk1-2* are auxin-insensitivity and
180 constitutive expression of PSI-genes[9,31-33]. Reduced $InsP_8$, common to *ipk1-1* or *itpk1-2*, likely
181 disrupt SPX1-PHR1 interactions leading to activation of PSI-genes[34]. MLN4924, a small
182 molecule pharmacological inhibitor of CUL neddylation[18] is functional in Arabidopsis, inhibits
183 degradation of CRL substrates and confers auxin insensitivity[35]. To test whether increased PSI-

184 gene expressions in *ipk1-1* or *itpk1-2* are consequences of enhanced CUL1-neddylation, we
185 treated these plants with MLN4924. Remarkably, elevated expression of PSI-genes such as
186 *PHT1;3, SPX1,* or *IPS1* as well as high endogenous Pi levels in *ipk1-1* or *itpk1-2* are reduced
187 upon MLN4924-treatment (Fig. 3a-b). In Col-0 grown under Pi-sufficient conditions,
188 MLN4924 treatments did not cause detectable change in endogenous Pi-levels or *IPS1*
189 expression (Fig. 3b; Extended Data Fig. 11). Most surprisingly, MLN4924 treatments
190 suppressed the induction of *PHT1;3* or *IPS1* in Col-0 when subjected to Pi-starvation (Fig. 3c).

191 To test whether neddylation efficiencies of cullins are affected upon Pi-deprivation, extracts
192 from Col-0 grown under Pi-replete or exposed to Pi-deplete conditions were immunoblotted
193 with anti-CUL1 antibodies. Prominent increase in $CUL1^{Nedd8}$ levels, sensitive to MLN4924
194 inhibition, was noted in Col-0 when shifted from Pi-replete to Pi-deplete conditions (Fig. 3d).
195 Basally enhanced levels of $CUL1^{Nedd8}$ in *ipk1-1* or *itpk1-2* remain unchanged under Pi-deplete
196 conditions (Extended Data Fig. 6). Surprisingly, enhancements of $CUL^{Nedd8}$ levels under Pi-
197 deplete conditions also occur in the PSR-defective *phr1phl1* plants implicating that neddylation
198 readjustments are upstream of PHR1/PHL1 (PHR1-LIKE 1) role in inducing PSI-gene
199 expressions (Fig. 3d). Our assays hence identify CUL1 hyperneddylation as an early response
200 to Pi-starvation essential to transduce downstream signaling.

201 Interestingly, in-lysate denddylation assay on Pi-starved Col-0 although shows diminished
202 CSN5 deneddylase activity, nevertheless unlike noted for *ipk1-1* or *itpk1-2*, CUL1 instabilities
203 are not accentuated (Extended Data Fig. 7). Also, CSN5 elution profiles under Pi-deplete
204 conditions are peculiarly similar to patterns in *ipk1-1* or *itpk1-2* with more engagements in the
205 CSN holo-complex fractions but no change in its total protein levels (Fig. 3e). Curiously, unlike
206 *ipk1-1* or *itpk1-2*, global ubiquitinylation are not enhanced upon Pi-starvation (Fig. 3f).
207 Together, these results indicate highly coordinated CRL-activities on substrates to maintain
208 specificity in responding to reduced Pi-availability. Combined, our data also suggest that Col-

209 0 plants tone-down CSN-deneddylase activity during Pi-deprivation to induce PSI-gene
210 expressions, a phenomenon that is constitutive in *ipk1-1* or *itpk1-2*. Overall fractionation
211 profiles of CSN1, or CUL1 remain unaltered by the Pi-changes (Extended Data Fig. 8a). We
212 also detect marked and modest increase in ITPK1-GFP and Myc-IPK1 protein levels,
213 respectively in Pi-starved extracts although their transcription efficiencies remain largely
214 unchanged[33] (Extended Data Fig. 8b). This is suggestive of possible modulations of their kinase
215 activities brought about by the increased accumulation and needs to be investigated further.
216 Together, with these observations, it is evident that CSN5 dynamics of the CSN is altered under
217 Pi-starvation.

218 **CSN5 loss or inhibition phenocopies *ipk1* or *itpk1* mutant responses.** To determine whether
219 PSI-gene expressions are globally affected by CSN functions, we mined the available
220 microarray data of differentially expressed transcripts in *csn* null mutants (*csn3*, *csn4* and
221 *csn5ab*)[36]. Strong upregulation in expressions compared to wild-type plants are especially
222 noted in genes responsible for Pi-remobilization (*PAP1, PAP10, PAP23, DFR, F3H*) and a few
223 Pi-transporters (*PHT3;2, PHT3;3, OCT1*), categorized earlier[31] (Extended Data Fig. 9).
224 Expressions of *PHR1* or *PHL1* remain unaffected as in *ipk1-1* or *itpk1-2* [31,32]. Neither *IPK1* nor
225 *ITPK1* transcriptions are changed in the *csn* mutants. Thus, CSN holo-complex defects overall
226 affect several PSI-gene expressions likely because of its deneddylation-deficiencies. To
227 explore CSN roles further, we utilized the *csn5a-2* plants (SALK_027705) harboring a T-DNA
228 insertion in the last exon of the *CSN5A* isoform (*At1g22920*). Similar to *ipk1-1* or *itpk1-2*,
229 *csn5a-2* extracts accumulate higher $CUL1^{Nedd8}$ levels and display auxin-insensitivity [9,29,30,36].
230 Under Pi-replete conditions, mild increase in basal Pi-levels accompanied by up-regulated
231 expressions of *PHT1;3* or *IPS1* is detected in the *csn5a-2* plants (Fig. 4a-b). These parallel
232 phenomena in *ipk1-1* or *itpk1-2*. Upon exposure to Pi-deplete conditions, and in contrast to
233 Col-0, *csn5a-2* plants are completely impaired in inducing *PHT1;3* or *IPS1* (Fig. 4b).

234 Strikingly, these results also resemble deficiencies in *itpk1-2* when subjected to Pi-starvation[33]
235 suggesting that CSN5 processes are linked to maintenance of Pi-homeostasis and successful
236 transduction of PSR.

237 To further substantiate CSN5 involvement, we tested the effects of recently reported CSN5
238 inhibitors Azaindole#6 and CSN5i-3 on Arabidopsis PSR[37,38]. In animal cell lines, these
239 inhibitors interfere with CSN5 deneddylase activity and trap CRLs in their neddylated states.
240 Because they remain untested in any plant systems, we first determined their efficacy on
241 Arabidopsis seedlings. Parallel MLN4924 treatments were used as neddylation-inhibition
242 controls. Dose-dependent increments in $CUL1^{Nedd8}$ levels with collateral decrease in
243 unneddylated-CUL1 are detected at 24hr post-treatment with CSN5i-3 (Fig. 4c). Even at 48-
244 hrs post-treatment, CSN5i-3 inhibitions are maintained (Extended Data Fig. 10). At all doses
245 tested, Azaindole#6 remained ineffective in changing $CUL1^{Nedd8}$: CUL1 ratios. As expected,
246 MLN4924 treatments in a dose-dependent manner reduce $CUL1^{Nedd8}$ levels. For subsequent
247 experiments, we continued with 10μM dose of CSN5i-3 and the same for MLN4924, as used
248 in earlier assays. On Col-0, CSN5i-3 caused a modest increase in basal Pi levels and
249 upregulation in expression of *PHT1;3*, but not significantly for *SPX1* or *IPS1*(Fig. 4d-e;
250 Extended Data Fig. 11a). Under Pi-deplete exposure, CSN5i-3 dramatically suppressed the
251 induction of *PHT1;3, SPX1* or *IPS1* in Col-0 and mirrored MLN4924 effects (Fig. 4e; Extended
252 Data Fi. 11a-b). CSN5i-3-treated Col-0 extracts when fractionated, CSN5 was clearly more
253 enriched in the CSN holo-complex pools resembling *ipk1-1*, *itpk1-2,* or Pi-starved profiles (Fig.
254 4f). With these results, we once again envision strong connection between CSN5 deneddylation
255 deficiencies in *ipk1-1* or *itpk1-2* plants to defects in CSN5 dynamics on CSN. Most
256 interestingly, *ipk1-1* or *itpk1-2* seedlings grown under sufficient Pi when treated with CSN5i-
257 3 have reduced *IPS1* expressions than untreated plants indicating that skewed kinetics of CSN5
258 rather complete deficiency in its functions is attributed to these mutants (Extended Data Fig.

259 11b). MLN4924-treatments on *ipk1-1* or *itpk1-2* in Pi-deplete growth medium offer relief by
260 elevating *IPS1* expressions further supporting our hypothesis that inadequacies in these
261 mutants to support PSR is related to dynamics of CSN5-regulated neddylation/deneddylation
262 cycles (Extended Data Fig. 11). From these results, it is imperative that IPK1/ITPK1 functions
263 influence CSN5 dynamics thus affecting the deneddylase activity of CSN holo-complex and
264 its role in executing PSR.

265 **ITPK1 activity primarily regulates CSN5 deneddylase functions of CSN.** $InsP_6$ rather than
266 $InsP_7$ is implicated as the physiological glue in potentiating CSN2-CRL associations[26]. That a
267 kinase-dead IP5K interacts weakly with CSN2/5 further implies that $InsP_6$ augmenting these
268 interactions is produced locally. Supplementing $InsP_6$ to IP5K-depleted cell lysates strengthens
269 CRL-CSN2 associations, and increases deneddylation rates of recombinant CSN on purified
270 neddylated cullins[26]. Apparently, the externally added metabolite gains access to its designated
271 binding pocket at the CRL-CSN2 interface. Even though CRL-CSN associations are not
272 affected in *ipk1-1* or *itpk1-2*, we investigated whether adding $InsP_6$ to lysates recover
273 deneddylation deficiencies in the mutants, or cause its augmentation in Col-0. Our results
274 clearly show that externally added $InsP_6$ does not alter deneddylation defects or CUL1
275 instability in *ipk1-1* or *itpk1-2* (Extended Data Fig. 12a). In Col-0 extracts, $InsP_6$
276 supplementation does not change deneddylation rates or stability of CUL1 indicating that
277 unlike mammalian systems, CSN functions in plants are not influenced by $InsP_6$.

278 Unlike $InsP_6$, the CRL-CSN release factor $InsP_7$ when supplemented to mammalian cell
279 extracts does not lead to complex disassembly[25]. This means that IP6K1 activity is very tightly
280 regulated spatiotemporally. With observed ITPK1-CSN2 interactions, this instigated us to
281 investigate whether CSN5 deneddylation deficiency in *ipk1-1* or *itpk1-2* is directly associated
282 with impaired ITPK1 activity. The cell-permeable compound TNP inhibits animal IP6K1
283 functions and reduce $InsP_7$ levels[39]. In 10μM TNP-treated Col-0 extracts, distinct increase in

284 CUL1$^{NEDD8}$ levels are observed although less potent to a similar dose of CSN5i-3 (Fig. 5a). We
285 used 25μM TNP doses for subsequent assays. In Col-0 grown in Pi-sufficient media, TNP
286 presence replicated CSN5i-3 results in augmenting basal Pi levels, upregulation of *IPS1* or
287 *SPX1* expressions, and more retention of CSN5 in the CSN holo-complex pools (Fig. 5b; Fig.
288 4f). TNP also suppressed endogenous deneddylation rates with increased CUL1 instability
289 (Fig. 5c). And likewise to CSN5i-3, TNP also suppressed PSI-gene inductions in Col-0 under
290 Pi-deplete circumstances (Fig. 5b). With these results, we provide convincing evidence of
291 ITPK1 activity-regulated CSN(5) implications in maintenance of Pi-homeostasis and PSR.
292 Overall, with our data we present localized coordinated activities of IPK1-ITPK1 pair in
293 modulating CSN dynamics, defining molecular concept of the CSN paradox, and underlining
294 CSN role in phosphate stress responses of plants.

295

296 **Discussion**

297 In animal systems, CRL-CSN tether is augmented by $InsP_6$ and released via stimulus-driven
298 $InsP_7$ synthesis. Here, we show that although Arabidopsis IPK1 and ITPK1 retain conserved
299 CSN interactions, $InsP_6$/$InsP_7$ changes in the corresponding mutants do not overall affect
300 CRL1-CSN associations. Thus, either the residual levels of these InsPs suffice at the CRL-CSN
301 junctures or the association/dissociation cycles involve an altogether different InsP(s) not
302 locally altered in the above mutants. That, unlike mammalian results, added $InsP_6$ does not
303 rescue *ipk1-1* or even alter CUL1 deneddylation rates/stability in Col-0 is supportive of strict
304 coordinated roles of IPK1-ITPK1 pair at CSN locales. Data showing an *ITPK4* mutant (*itpk4-*
305 *1*) with reduced $InsP_6$/$InsP_7$ as *ipk1-1* or *itpk1-2* has normal PSR[32] and Col-0 comparable ratio
306 of CUL1$^{Nedd8}$:CUL1 (Extended Data Fig. 12b) also lends support to our hypothesis. However,
307 in one striking distinction both *ipk1-1* or *itpk1-2* accumulate increased levels of Ins(3,4,5,6)$P_4$

308 which neither the *itpk4-1* nor Col-0 subjected to PSR does[32]. Whether the recently reported
309 reversibility of Ins(3,4,5,6)$P_4$ to Ins$P_7$ synthesis catalyzed by substrate-product related IPK1-
310 ITPK1 pair and strongly influenced by cellular energy status in principle affects CSN functions
311 need to be investigated further[33,40,41]. In all regards, our model (Fig.5e) proposing that
312 decreased CSN5 deneddylase performance and lower CUL1 deneddylation rates due to loss of
313 IPK1 or ITPK1 nevertheless implicates their activities in CSN roles on CRLs. With previously
314 known effects of mammalian ITPK1 over-expression on CSN5 equilibrium [28], we show here
315 the similar phenomenon in absence/upon inhibition of either ITPK1 or CSN5 revealing
316 intricately choreographed plant ITPK1 role on CSN5 dynamics especially its entry-exit shuttles
317 and deneddylase activity.

318 With obvious Ins$P_8$ reduction in *ipk1-1*, *itpk1-2* or upon Pi-starvation, PHR1 liberated from
319 SPX1 causes activation of PSI-gene expressions. In turn, SPXs undergo ubiquitination by
320 homologs of recently identified rice ubiquitin E3 ligases SDEL1/2[13,14,17,42]. Here we
321 demonstrate that perception of Pi-deprivation is accompanied by PHR1/PHL1-independent
322 increase in CUL1 neddylation, a feature mimicked constitutively by ITPK1 loss/inhibition and
323 suppressed by the neddylation inhibitor MLN4924. Pronounced CSN5 retentions on CSN holo-
324 complex along with dampened deneddylation rates facilitate more available pools of
325 neddylated CRLs to ubiquitinylate SPX1 and other substrates. This is evident from
326 constitutively enhanced global pool of ubiquitinylated proteins in *ipk1-1* or *itpk1-2* extracts. In
327 Pi-starved plants, this ubiquitinylation is tightly regulated and restricted to intended substrates,
328 such as SPX1, without notably changing global polyubiquitin-conjugates. Failure to respond
329 under low-Pi and induce PSI-gene upregulations in *itpk1-2*[33] or by inhibition of ITPK1 or
330 CSN5, indicates that the observed CSN5 partitioning changes upon Pi-starvation is only a
331 transitory shift of deneddylase kinetics, and not complete inhibition of its activity. And CRLs
332 continue to require neddylation/deneddylation cycles to successfully transduce PSR. This again

333 may be linked to InsPs generated by reverse reactions of IPK1-ITPK1 pair under changed
334 adenylate charge as occurring during Pi-starvation[33,40]. Overall, with our data we highlight
335 IPK1-ITPK1 role in CSN regulations that addresses key aspects of its multi-faceted functions
336 in responding to Pi-imbalances.

337

338 **References**


339 1 Raboy, V. Accumulation and Storage of Phosphate and Minerals. *Cellular and*
340 *Molecular Biology of plant Seed Development*, 441-477, doi:10.1007/978-94-015-
341 8903-3_12 (1997).
342 2 Stevenson-Paulik, J., Bastidas, R. J., Chiou, S. T., Frye, R. A. & York, J. D. Generation
343 of phytate-free seeds in Arabidopsis through disruption of inositol polyphosphate
344 kinases. *Proc Natl Acad Sci U S A* **102**, 12612-12617, doi:10.1073/pnas.0504172102
345 (2005).
346 3 Monserrate, J. P. & York, J. D. Inositol phosphate synthesis and the nuclear processes
347 they affect. *Curr Opin Cell Biol* **22**, 365-373, doi:10.1016/j.ceb.2010.03.006 (2010).
348 4 Shears, S. B. & Wang, H. Inositol phosphate kinases: Expanding the biological
349 significance of the universal core of the protein kinase fold. *Adv Biol Regul* **71**, 118-
350 127, doi:10.1016/j.jbior.2018.10.006 (2019).
351 5 Desai, M. *et al.* Two inositol hexakisphosphate kinases drive inositol pyrophosphate
352 synthesis in plants. *Plant J* **80**, 642-653, doi:10.1111/tpj.12669 (2014).
353 6 Adepoju, O. *et al.*, doi:10.1101/724914 (2019).
354 7 Laha, D. *et al.* VIH2 Regulates the Synthesis of Inositol Pyrophosphate InsP8 and
355 Jasmonate-Dependent Defenses in Arabidopsis. *Plant Cell* **27**, 1082-1097,
356 doi:10.1105/tpc.114.135160 (2015).

357 8 Laha, D. *et al.* Arabidopsis ITPK1 and ITPK2 Have an Evolutionarily Conserved Phytic
358 Acid Kinase Activity. *ACS Chem Biol* **14**, 2127-2133,
359 doi:10.1021/acschembio.9b00423 (2019).
360 9 Laha, N. P. *et al.*, ITPK1-Dependent Inositol Polyphosphates Regulate Auxin
361 Responses in *Arabidopsis thaliana*. *BioRxiv preprint* doi:10.1101/2020.04.23.058487
362 (2020).
363 10 Sheard, L. B. *et al.* Jasmonate perception by inositol-phosphate-potentiated COI1-JAZ
364 co-receptor. *Nature* **468**, 400-405, doi:10.1038/nature09430 (2010).
365 11 Tan, X. *et al.* Mechanism of auxin perception by the TIR1 ubiquitin ligase. *Nature* **446**,
366 640-645, doi:10.1038/nature05731 (2007).
367 12 Bustos, R. *et al.* A central regulatory system largely controls transcriptional activation
368 and repression responses to phosphate starvation in Arabidopsis. *PLoS Genet* **6**,
369 e1001102, doi:10.1371/journal.pgen.1001102 (2010).
370 13 Lv, Q. *et al.* SPX4 Negatively Regulates Phosphate Signaling and Homeostasis through
371 Its Interaction with PHR2 in Rice. *Plant Cell* **26**, 1586-1597,
372 doi:10.1105/tpc.114.123208 (2014).
373 14 Osorio, M. B. *et al.* SPX4 Acts on PHR1-Dependent and -Independent Regulation of
374 Shoot Phosphorus Status in Arabidopsis. *Plant Physiol* **181**, 332-352,
375 doi:10.1104/pp.18.00594 (2019).
376 15 Puga, M. I. *et al.* SPX1 is a phosphate-dependent inhibitor of Phosphate Starvation
377 Response 1 in Arabidopsis. *Proc Natl Acad Sci U S A* **111**, 14947-14952,
378 doi:10.1073/pnas.1404654111 (2014).
379 16 Rubio, V. *et al.* A conserved MYB transcription factor involved in phosphate starvation
380 signaling both in vascular plants and in unicellular algae. *Genes Dev* **15**, 2122-2133,
381 doi:10.1101/gad.204401 (2001).

382 17 Zhong, Y. *et al.* Rice SPX6 negatively regulates the phosphate starvation response
383 through suppression of the transcription factor PHR2. **219**, 135-148,
384 doi:10.1111/nph.15155 (2018).
385 18 Soucy, T. A. *et al.* An inhibitor of NEDD8-activating enzyme as a new approach to
386 treat cancer. *Nature* **458**, 732-736, doi:10.1038/nature07884 (2009).
387 19 Yi Sun, W. W., Jianping Jin. <CRL Book Sun etal 2020.pdf>. *Advances in*
388 *Experimental Medicine and Biology Biology and Therapeutics* **1217**, doi:10.1007/978-
389 981-15-1025-0 (2020).
390 20 Chamovitz, D. A. & Segal, D. JAB1/CSN5 and the COP9 signalosome. A complex
391 situation. **2**, 96-101, doi:10.1093/embo-reports/kve028 (2001).
392 21 Dubiel, D., Rockel, B., Naumann, M. & Dubiel, W. Diversity of COP9 signalosome
393 structures and functional consequences. *FEBS Lett* **589**, 2507-2513,
394 doi:10.1016/j.febslet.2015.06.007 (2015).
395 22 Cope, G. A. *et al.* Role of predicted metalloprotease motif of Jab1/Csn5 in cleavage of
396 Nedd8 from Cul1. *Science* **298**, 608-611, doi:10.1126/science.1075901 (2002).
397 23 Dubiel, W. Resolving the CSN and CAND1 paradoxes. *Mol Cell* **35**, 547-549,
398 doi:10.1016/j.molcel.2009.08.011 (2009).
399 24 Lin, H. *et al.* Basis for metabolite-dependent Cullin-RING ligase deneddylation by the
400 COP9 signalosome. *Proc Natl Acad Sci U S A* **117**, 4117-4124,
401 doi:10.1073/pnas.1911998117 (2020).
402 25 Rao, F. *et al.* Inositol hexakisphosphate kinase-1 mediates assembly/disassembly of the
403 CRL4-signalosome complex to regulate DNA repair and cell death. *Proc Natl Acad Sci*
404 *U S A* **111**, 16005-16010, doi:10.1073/pnas.1417900111 (2014).

405 26 Scherer, P. C. *et al.* Inositol hexakisphosphate (IP6) generated by IP5K mediates cullin-
406 COP9 signalosome interactions and CRL function. *Proc Natl Acad Sci U S A* **113**, 3503-
407 3508, doi:10.1073/pnas.1525580113 (2016).
408 27 Qin, Z. X., Chen, Q. J., Tong, Z. & Wang, X. C. The Arabidopsis inositol 1,3,4-
409 trisphosphate 5/6 kinase, AtItpk-1, is involved in plant photomorphogenesis under red
410 light conditions, possibly via interaction with COP9 signalosome. **43**, 947-954,
411 doi:10.1016/j.plaphy.2005.08.006 (2005).
412 28 Sun, Y., Wilson, M. P. & Majerus, P. W. Inositol 1,3,4-trisphosphate 5/6-kinase
413 associates with the COP9 signalosome by binding to CSN1. *J Biol Chem* **277**, 45759-
414 45764, doi:10.1074/jbc.M208709200 (2002).
415 29 Dohmann, E. M., Kuhnle, C. & Schwechheimer, C. Loss of the CONSTITUTIVE
416 PHOTOMORPHOGENIC9 signalosome subunit 5 is sufficient to cause the cop/det/fus
417 mutant phenotype in Arabidopsis. *Plant Cell* **17**, 1967-1978,
418 doi:10.1105/tpc.105.032870 (2005).
419 30 Gusmaroli, G., Feng, S. & Deng, X. W. The Arabidopsis CSN5A and CSN5B subunits
420 are present in distinct COP9 signalosome complexes, and mutations in their JAMM
421 domains exhibit differential dominant negative effects on development. *Plant Cell* **16**,
422 2984-3001, doi:10.1105/tpc.104.025999 (2004).
423 31 Kuo, H. F. *et al.* Arabidopsis inositol pentakisphosphate 2-kinase, AtIPK1, is required
424 for growth and modulates phosphate homeostasis at the transcriptional level. *Plant J*
425 **80**, 503-515, doi:10.1111/tpj.12650 (2014).
426 32 Kuo, H. F. *et al.* Arabidopsis inositol phosphate kinases IPK1 and ITPK1 constitute a
427 metabolic pathway in maintaining phosphate homeostasis. *Plant J*,
428 doi:10.1111/tpj.13974 (2018).

429 33 Riemer, E. *et al.*, ITPK1 is an InsP6/ADP phosphotransferase that controls systemic
430 phosphate homeostasis in Arabidopsis. *BioRxiv preprint*
431 doi:10.1101/2020.05.18.100297 (2020).
432 34 Ried, M. K. *et al.*, Inositol pyrophosphates promote the interaction of SPX domains
433 with the coiled-coil motif of PHR transcription factors to regulate plant phosphate
434 homeostasis *BioRxiv preprint* doi:10.1101/2019.12.13.875393 (2019).
435 35 Hakenjos, J. P. *et al.* MLN4924 is an efficient inhibitor of NEDD8 conjugation in
436 plants. *Plant Physiol* **156**, 527-536, doi:10.1104/pp.111.176677 (2011).
437 36 Dohmann, E. M., Levesque, M. P., Isono, E., Schmid, M. & Schwechheimer, C. Auxin
438 responses in mutants of the Arabidopsis CONSTITUTIVE PHOTOMORPHOGENIC9
439 signalosome. *Plant Physiol* **147**, 1369-1379, doi:10.1104/pp.108.121061 (2008).
440 37 Altmann, E. *et al.* Azaindoles as Zinc-Binding Small-Molecule Inhibitors of the JAMM
441 Protease CSN5. *Angew Chem Int Ed Engl* **56**, 1294-1297, doi:10.1002/anie.201608672
442 (2017).
443 38 Schlierf, A. *et al.* Targeted inhibition of the COP9 signalosome for treatment of cancer.
444 *Nat Commun* **7**, 13166, doi:10.1038/ncomms13166 (2016).
445 39 Padmanabhan, U., Dollins, D. E., Fridy, P. C., York, J. D. & Downes, C. P.
446 Characterization of a selective inhibitor of inositol hexakisphosphate kinases: use in
447 defining biological roles and metabolic relationships of inositol pyrophosphates. *J Biol*
448 *Chem* **284**, 10571-10582, doi:10.1074/jbc.M900752200 (2009).
449 40 Whitfield, H. *et al.* An ATP-responsive metabolic cassette comprised of inositol
450 tris/tetrakisphosphate kinase 1 (ITPK1) and inositol pentakisphosphate 2-kinase (IPK1)
451 buffers diphosphosphoinositol phosphate levels. *Biochem J* **477**, 2621-2638,
452 doi:10.1042/BCJ20200423 (2020).

453 41 Wundenberg, T. & Mayr, G. W. Synthesis and biological actions of diphosphoinositol
454 phosphates (inositol pyrophosphates), regulators of cell homeostasis. *Biol Chem* **393**,
455 979-998, doi:10.1515/hsz-2012-0133 (2012).
456 42 Ruan, W. *et al.* Two RING-Finger Ubiquitin E3 Ligases Regulate the Degradation of
457 SPX4, An Internal Phosphate Sensor, for Phosphate Homeostasis and Signaling in Rice.
458 *Mol Plant* **12**, 1060-1074, doi:10.1016/j.molp.2019.04.003 (2019).
459 43 Enchev, R. I. *et al.* Structural basis for a reciprocal regulation between SCF and CSN.
460 *Cell Rep* **2**, 616-627, doi:10.1016/j.celrep.2012.08.019 (2012).
461 44 Mosadeghi, R. *et al.* Structural and kinetic analysis of the COP9-Signalosome
462 activation and the cullin-RING ubiquitin ligase deneddylation cycle. *Elife* **5**,
463 doi:10.7554/eLife.12102 (2016).
464 45 Jia, X., Chanda, B., Zhao, M., Brunner, A. M. & Beers, E. P. Instability of the
465 Arabidopsis mutant csn5a-2 caused by epigenetic modification of intronic T-DNA.
466 **238**, 53-63, doi:10.1016/j.plantsci.2015.05.015 (2015).
467 46 Bhattacharjee, S., Halane, M. K., Kim, S. H. & Gassmann, W. Pathogen effectors target
468 Arabidopsis EDS1 and alter its interactions with immune regulators. *Science* **334**, 1405-
469 1408, doi:10.1126/science.1211592 (2011).
470 47 Chakrabarty, R. *et al.* PSITE vectors for stable integration or transient expression of
471 autofluorescent protein fusions in plants: probing Nicotiana benthamiana-virus
472 interactions. *Mol Plant Microbe Interact* **20**, 740-750, doi:10.1094/MPMI-20-7-0740
473 (2007).
474 48 Huang, H., Quint, M. & Gray, W. M. The eta7/csn3-3 auxin response mutant of
475 Arabidopsis defines a novel function for the CSN3 subunit of the COP9 signalosome.
476 *PLoS One* **8**, e66578, doi:10.1371/journal.pone.0066578 (2013).

477 49 Kim, S. H. *et al.* The Arabidopsis resistance-like gene SNC1 is activated by mutations
478 in SRFR1 and contributes to resistance to the bacterial effector AvrRps4. *PLoS Pathog*
479 **6**, e1001172, doi:10.1371/journal.ppat.1001172 (2010).
480 50 Chiou, T. J. *et al.* Regulation of phosphate homeostasis by MicroRNA in Arabidopsis.
481 *Plant Cell* **18**, 412-421, doi:10.1105/tpc.105.038943 (2006).

482

483 **Figure legends**

484 **Fig. 1. IPK1 and ITPK1 interact with each other and with selective CSN or CRLs**
485 **components *in planta*. a-b,** Immuno-enrichments of IPK1 **(a)** or ITPK1 **(b)** from
486 corresponding complemented lines (*ipk1-1: Myc-IPK1* or *itpk1-2:ITPK1-GFP*, respectively)
487 and probed with anti-CSN1/2/4/5, anti-CUL1, or anti-ASK1 antibodies. IgG-agarose
488 enrichments were used as negative controls. **c-d,** Bimolecular Fluorescence Complementation
489 (BiFC) assays showing reciprocal combinations of **(c)** IPK1 and **(d)** ITPK1 interact with CSN1.
490 Scale bar=50 μm. **e,** Co-immunoprecipitation of transiently expressed GFP-ITPK1 with Myc-
491 IPK1. Immuno-enrichment was performed with anti-GFP antibody-conjugated agarose and
492 probed with anti-GFP or anti-Myc antibodies. **f,** *In vitro* interactions of IPK1 with ITPK1. $His_6$-
493 IPK1 was co-expressed with GST alone or GST-ITPK1 in *E. coli* cells. $Ni^{2+}$NTA-affinity
494 enrichments were probed for $His_6$-IPK1 or GST-ITPK1 with anti-His or anti-GST antibodies,
495 respectively. Migration positions of molecular weight markers (in kDa) and of $His_6$-IPK1, GST
496 or GST-ITPK1 are shown on the right or left of each panel, respectively.

497 **Fig. 2. CSN5 partitioning and deneddylase functions are affected in *ipk1-1* or *itpk1-2*. a,**
498 IPK1 or ITPK1 does not co-elute with the CSN holo-complex. **b,** CRL1 fractionation profiles
499 are unchanged between Col-0, *ipk1-1* and *itpk1-2*. **c,** Enhanced CSN5 engagement on CSN
500 holo-complex fractions in *ipk1-1* and *itpk1-2*. For fractionations, extracts were separated by

501 size-exclusion chromatography and immuno-blotted with indicated antibodies. Right panels
502 are immunoblots on input extracts. Fraction numbers are indicated above each lane. Numbers
503 above arrowheads denote elution positions of molecular weight standards (in kDa). **d,**
504 Increased neddylated CUL1 in *ipk1-1* or *itpk1-2*. **e,** Global polyubiquitin-conjugates are
505 enhanced in *ipk1-1* or *itpk1-2*. For **d-e**, Total protein extracts were probed with anti-CUL1,
506 anti-actin, or anti-Ubiquitin antibodies as indicated. **f,** CSN5-deneddylation deficiencies and
507 lower CUL1 half-life in *ipk1-1* or *itpk1-2*. For in-lysate deneddylation assay total protein
508 extracts incubated for indicated times (minutes post-incubation; mpi) were probed with anti-
509 CUL1 antibodies. Migration position of molecular weight standards (in kDa) and neddylated
510 ($CUL1^{Nedd8}$) or unneddylated (CUL1) cullin1 are shown. Anti-actin or Ponceau S staining
511 demonstrate loadings controls.

512 **Fig. 3. CUL1 deneddylation rates are reduced during Pi-starvation.** MLN4924 suppresses
513 **a,** elevated PSI-gene expressions, and **b,** reduces endogenous Pi-levels in *ipk1-1* or *itpk1-2*. **c,**
514 MLN4924 suppresses the induction of *PHT1;3* or *IPS1* expressions in Col-0 upon Pi-
515 starvation. **d,** Enhanced CUL1-neddylation during Pi-deprivation is PHR1/PHL1-independent.
516 **e,** Increased CSN5 partitioning on CSN holo-complex occur upon Pi-starvation. **f,** Global levels
517 of polyubiquitin-conjugates are unperturbed during PSR. Gene expression changes were
518 relative to *MON1* transcripts and reported as fold-change relative to Col-0 levels. Data is
519 presented as mean $\pm$ SD (n=3 biological replicates of 3 plants in each). For Pi-estimation
520 assays, data shown as mean $\pm$ SD (n= 6-7 plants). Asterisks denote significant differences from
521 the reference sample. (Student's *t*-test; $*P<0.05$, $**P < 0.01$; $***P < 0.001$, $***P<0.0001$. ns
522 is not significant). For immunoblots, total protein extracts or fractions were probed with anti-
523 CUL1 or anti-CSN5 or anti-ubiquitin antibodies, as indicated. Ponceau S staining show
524 loadings controls. For Pi-deprivation/MLN4924 treatment assays, Seedlings grown in Pi-
525 replete (625μM Pi) medium were either maintained or transferred to Pi-deplete (10 μM Pi)

526 medium for three additional days in the presence of MLN4294 or absence (DMSO) during the
527 shift, before being analyzed. Positions of molecular weight markers (in kDa) are shown.

528 **Fig. 4. The dynamics of CSN5 is essential for responding to phosphate-starvation. a,**
529 *csn5a-2* plants have elevated endogenous Pi levels. **b,** *csn5a-2* plants are deficient in inducing
530 PSI-genes during Pi-starvation. **c,** CSN5i-3 shows dose-dependent inhibition in CUL1
531 deneddylation. Total protein extracts from Col-0, 24hrs post-treated with indicated doses of the
532 inhibitors mentioned, were probed with anti-CUL1 antibodies. Ponceau S staining shows
533 loading controls. **d,** CSN5i-3 treatment elevates endogenous Pi-levels. **e,** CSN5i-3 suppresses
534 *PHT1;3* induction in Col-0 during phosphate-starvation. **f,** CSN5 is enriched in CSN holo-
535 complex pools upon CSN5i-3 or TNP treatment. Fractionation was performed 24hrs post-
536 inhibitor treatment and fractions immunoblotted with anti-CSN5 antibodies. For Pi-estimation
537 assays, error bars show SD from mean (n=3 replicates of 5-6 plants each). For gene expression
538 changes, *MON1* levels were used as internal controls and results reported as fold-change
539 relative to untreated Pi-replete grown Col-0. Data is mean $\pm$ SD (n=3 replicates, 3-4 plants
540 each). Statistical significance was calculated with Student's *t*-test and depicted with $*P<0.05$,
541 $**P < 0.01$; $***P < 0.001$, $***P<0.0001$. ns is not significant. For Pi-deprivation assays, plants
542 grown in Pi-replete (625µM Pi) media were transferred for 3 days to Pi-deplete (10 µM Pi)
543 media with or without indicated inhibitors before analysis.

544 **Fig. 5. ITPK1 activity regulates CSN5 dynamics and deneddylase functions. a,** TNP
545 treatment enhances pools of neddylated CUL1. Total protein extracts from Col-0 at 24hrs post-
546 inhibitor treatment were immunoblotted with anti-CUL1 antibodies. **b,** TNP treatments
547 increase endogenous Pi-content in Col-0. Error bars are mean $\pm$ SD (n=3 replicates of 5-6 plants
548 each). **c,** TNP suppresses *IPS1* or *SPX1* in Col-0 upon Pi-starvation. For Pi-starvation, plants
549 grown in Pi-replete medium were transferred for 3 days to Pi-deplete medium with or without
550 TNP. Expression levels of *MON1* transcripts was used as internal reference. Error bars denote

551 mean with SD (n=3 biological replicates of 3-4 plants each). Student's *t*-test was used to
552 calculate statistical significance and shown as $^{**}P<0.01$, $^{***}P<0.001$, $^{****}P<0.0001$, ns not
553 significant. **d,** TNP reduces CUL1 deneddylation and increases CUL1 instability. In-lysate
554 deneddylation assay on Col-0 extracts post-24hrs TNP-treatment and then probed with anti-
555 CUL1 antibodies. Ponceau S staining indicates loadings control. **e,** Schematic representation
556 of IPK1-ITPK1 role on CRL-CSN association/dissociation equilibrium in plants. CSN holo-
557 complex platform offers protection to CRLs in absence of ubiquitinylation substrates (E2
558 enzyme prevented from binding due to mutual exclusion[43,44]) utilizing coordinated locale-
559 specific activities (bi-directional white arrows) of IPK1 and ITPK1. Stimulus/energy status-
560 dependent modulation in localized IPK1/ITPK1 activities (InsPs nature unknown; red question
561 mark) is coupled to CRL, CSN5 disassembly and CUL1 deneddylation. Auto-inhibited CSN
562 holo-complex is reconstituted by re-incorporating CSN5. Active CRL-SCF complex binds E2
563 ubiquitin enzyme to cause targeted ubiquitinylation ($Ub^n$) and degradation of substrates (such
564 as SPX1 or Aux/IAA repressors). Inhibitory functions of TNP, CSN5i-3 and MLN4924 are
565 indicated on the respective processes. CSN subunits are presented as numbers; CUL1, Cullin1;
566 RBX, RING H2 protein1; SA, substrate adapter, N8, Nedd8, IPK1, inactive IPK1, ITPK1,
567 inactive ITPK1, IPK1 InsP, active IPK1, ITPK1 InsP, active ITPK1.

568

569 **Methods**

570 **Plant material and growth conditions.** Seeds of T-DNA insertion lines of *Arabidopsis*
571 *thaliana* (ecotype Col-0) were obtained from the Arabidopsis Biological Resource Center
572 (ABRC). Homozygous *ipk1-1* (SALK_065337[31]), *itpk1-2* (SAIL_65_D03[32]) *ipk2β-1*
573 (SALK_104995[2]) and *csn5a-2* (SALK_027705[45]) were genotyped using T-DNA and
574 respective gene-specific primers listed in Supplementary Table 1. The *vih2-4, itpk1-2:ITPK1-*

575 *GFP,* and *phr1 phl1* plants have been reported earlier[9,31,32]. Seeds were stratified for 2-days at
576 4°C in dark and then sterilized using 30% bleach solution. They were germinated either directly
577 on soil or on ½ strength Murashige and Skoog (MS) Pi-replete (625 μM $KH_2PO_4$) agar plates
578 in growth chambers maintained at 22°C with 70% Relative humidity (RH) and 16hrs: 8hrs;
579 light: dark having light intensity 100 μmol $\mu m^{-2}s^{-1}$. For fractionation, Pi-starvation assays, and
580 inhibitor treatments, plants grown on media plates as above were transferred 7-days post-
581 germination to liquid ½ MS medium in 12-well sterile culture plates are proceeded accordingly
582 as indicated in respective experiments. For immuno-precipitation assays 4-week-old soil-
583 grown plants were used.

584 **Generation of constructs.** Arabidopsis *IPK1*, *ITPK1*, *CSN1* and *CSN2* cDNAs were amplified
585 via RT-PCR (iScript cDNA Synthesis Kit, Bio-Rad, USA) from total RNA isolated using
586 RNAiso (Takara-Bio, Japan) from 2-week-old Col-0 plants. Primers for these are listed in
587 Supplementary Table 1. Gateway cloning was first performed into *p*DONR 207 and then into
588 *p*BA-Myc[46] (for Myc-IPK1), *p*SITE-2CA[47] (for GFP-ITPK1), nVenus- or cCFP binary
589 vectors[46] (for all the above) using BP and LR Clonase, respectively (Invitrogen, USA). BiFC
590 vectors for GUS expression have been described earlier[46]. The clones were confirmed by
591 sequencing and electroporated into the agrobacterium strain GV3101 for further assays. For
592 generating clones for recombinant protein expression and *in vitro* interaction assays, IPK1 was
593 sub-cloned into *p*ET28a as *BamH*I-*Sal*I fragment while ITPK1 was cloned as into *p*GEX4T-3
594 as *BamH*I-*Xho*I fragment (primers listed in Supplementary Table 1) to generate $His_6$-IPK1 and
595 GST-ITPK1, respectively.

596 **Bimolecular Fluorescence Complementation (BiFC) assays.** Agrobacterium strains
597 containing the indicated combination of binary vectors were co-infiltrated at equal cell
598 densities into mature *Nicotiana benthamiana* leaves. After 48hrs post-infiltration, tissue

599 sections from the infiltrated patches were viewed under a SP8 confocal microscope (Leica-
600 microsystems, Germany). Images were acquired with both bright field and YFP filters.

601 ***In vitro* interaction assays in *E. coli*.** Bacterial strain BL21-AI (Arabinose inducible;
602 Thermofisher, USA) harboring GST-ITPK1 or GST with $His_6$-IPK1 plasmids was grown to
603 0.4 $OD_{600nm}$, induced with 0.1M IPTG and 0.2% L-arabidose overnight at 28$^{o}$C. Cell pellets
604 were processed according to manufacturer's instructions, bound to $Ni^{2+}$-NTA beads (Qiagen,
605 Germany) for 3hrs at 4$^{o}$C with tumbling, washed and eluted with imidazole. Imidazole was
606 removed via dialysis and elute was immuno-blotted with anti-His or anti-GST antibodies.

607 **Generation of transgenic lines.** For generating complemented *ipk1-1:Myc-IPK1*
608 complemented line, *ipk1-1* plants were floral-dipped with the agrobacterium strain containing
609 Myc-IPK1 binary vector. Transgenic plants were selected on phosphinothricin (10μg/ml)
610 containing ½ MS agar plates and propagated to homozygosity and then used for indicated
611 assays.

612 **Pull down assay/Immunoprecipitation assays.** For co-immunoprecipitation assays between
613 Myc-IPK1 and GFP-ITPK1, agro-infiltrated *N. benthamiana* leaves harvested at 48hrs post-
614 infiltration were used. For pull-downs, including from Arabidopsis transgenic lines *ipk1-*
615 *1:Myc-IPK1*, and *itpk1-2:ITPK1-GFP*, extracts were homogenized in cold RIPA buffer [5mM
616 Tris-HCl pH 7.5, 150mM NaCl, 10mM $MgCl_2$, 1mM EDTA, 1% NP-40, 1mM Sodium
617 deoxycholate and 1X protease inhibitor cocktail (Sigma-Aldrich, USA)]. After removing cell
618 debris via centrifugation, the supernatant was pre-cleared with IgG agarose beads (Sigma-
619 Aldrich, USA) at 4$^{o}$C for 1hr with rotation. The mix was then centrifuged, IgG agarose bead-
620 pellet washed and saved as non-specific controls. The supernatant was added to indicated
621 antibody-conjugated beads (anti-GFP Agarose, BioBharati Life Sciences, India; anti-Myc
622 Agarose, Sigma-Aldrich, USA). After tumbling overnight at 4$^{o}$C, the mix was centrifuged, and

623 agarose-bead pellet washed 3-times with RIPA buffer. Beads were then resuspended in 1X
624 Laemmli loading dye and used for immunoblots. For CUL1 pull-down, anti-CUL1 antibodies
625 were first bound to Protein A/G agarose (Sigma-Aldrich, USA), washed and then incubated
626 with Arabidopsis extracts prepared in RIPA buffer as above. Binding was allowed overnight at
627 $4^{o}C$ with rotation, washed next day as earlier and processed for immunoblots.

628 **Size-exclusion chromatography of plant extracts.** Gel-filtration protocol was according to
629 Huang et al (2013)[48]. Briefly, 14-day-old plants ground to a fine powder with liquid nitrogen
630 were homogenized in Gel filtration buffer (50mM Tris-HCl pH 7.5, 150mM NaCl, 1mM
631 EDTA, 10% Glycerol, 10mM $MgCl_2$, 1mM DTT, 1mM PMSF and 1X Protease inhibitor
632 cocktail). Homogenates were centrifuged for 10 mins at $4^{o}C$ and supernatant passed through
633 0.2 μM syringe filters. Total protein extracts were fractionated through Superdex 10/300 GL
634 Column (GE- Healthcare, USA) and eluted in the fractionation buffer at 0.2mL/min flow rate.
635 The eluants were TCA (Trichloroacetic acid) precipitated, washed with acetone and
636 resuspended in 1X Laemmli loading dye and used for indicated immunoblots.

637 **qRT-PCR analysis.** cDNAs prepared as earlier, were used for qRT-PCRs with HOT FIREPol
638 EvaGreen qPCR Mix Plus (ROX) (Solis BioDyne, USA) and primer combinations according
639 to the manufacturer's instructions. Primers used are listed in Supplementary Table 1. Reaction
640 was performed on QuantStudio 6 Flex Real-Time PCR system (Applied Biosystems, USA)
641 with three biological and technical replicates. *MON1* (*At2g28390*) expressions were used as
642 internal control[49]. Relative expression was calculated according to the PCR efficiency^-ΔΔCt
643 formula.

644 **Protein extraction and immunoblots.** Total protein extracts from plants were prepared in 6M
645 Urea and used for western blots. For immunodetection, anti-GFP, anti-Myc (BioBharati Life
646 Sciences, India), anti-CSN1, anti-CSN2, anti-CSN4, anti-CSN5, anti-ASK1, anti-CUL1

647 antibodies (ENZO Life Sciences, USA), anti-Actin (Abiocode, USA) were used. The blots
648 were developed using ECL kit (Bio-Rad, USA) and developed in Alpha Image Quant system
649 (GE-Healthcare, USA).

650 **In-lysate deneddylation assay.** In-lysate deneddylayion assay was according to Lin et al
651 (2020)[24]. Briefly, 14-day-old seedlings were quickly homogenized in deneddylayion buffer
652 (10mM Tris-HCl pH7.5, 150mM NaCl and 0.5% NP-40) in absence of protease inhibitors. The
653 extracts were incubated at 37$^{o}$C for indicated times, reaction stopped by adding Laemmli
654 loading dye to 1X, and then used for immunoblots.

655 **Pi-estimation assay.** Total Pi measurements is according to Chiou et al (2006)[50]. In brief, fresh
656 tissue was frozen with liquid nitrogen and homogenized in extraction buffer (10mM Tris-HCl,
657 1mM EDTA, 100mM NaCl, 1mM PMSF). The homogenized sample was mixed in a ratio of
658 1:9 with 1% glacial acetic acid and incubated at 42$^{o}$C for 30mins. Then the reaction was mixed
659 in a ratio of 3:7 with Pi-assay solution (0.35% $NH_4MoO_4$, 0.86N $H_2SO_4$ and 1.4% ascorbic
660 acid) and incubated at 42$^{o}$C for 30mins. Pi content was measured at A280 using a
661 spectrophotometer. Standard graph was made with known amounts of $KH_2PO_4$.

662 **Phosphate-starvation assays.** After germination of seeds as described earlier, seedlings were
663 transferred to liquid ½ MS medium in 12-well sterile culture plates with Pi-replete conditions
664 (625 μM $KH_2PO_4$) and placed in the growth chamber. After 4-days, the plants were either
665 maintained with Pi-replete or transferred to Pi-deplete (10 μM $KH_2PO_4$) liquid media and
666 continued for another 3 days (total 14-days post-germination) before being used for Pi-
667 estimation, qRT-PCR, total protein extraction, fractionation assays.

668 **Inhibitor treatments.** Stock solutions of MLN4924 (Cayman Chemicals, USA), CSN5i-3
669 (Novartis Inc, Switzerland), or TNP (Sigma-Aldrich, USA) was prepared in DMSO. For
670 treatments, 10μM final concentration of MLN4924 or CSN5i-3 were used. TNP was used at

671 25μM final unless otherwise indicated. For assays on Col-0, *ipk1-1*, or *itpk1-2* or for
672 fractionations, inhibitors were treated for 24hrs. For effects on PSR, inhibitors were added
673 during the shift to Pi-deplete medium.

674 **Ubiquitination assays.** For determining global ubiquitination levels, extracts from indicated
675 plants prepared in Gel filtration buffer in the presence of 10μM proteasome inhibitor MG132
676 were incubated on ice for 2hrs. Immunoblotting was then performed with anti-ubiquitin
677 antibodies (P4D1; SantaCruz Biotechnology, USA).

678 **Statistical analysis.** All Data presented here are representative of at least three biological and
679 technical replicates for each. Student's *t*-test were applied for statistical analysis.

680

681 **Acknowledgements**

682 We thank Regional Centre for Biotechnology (RCB), Faridabad, for financial support, lab
683 infrastructure, and central instrumental facilities. S.B. expresses gratitude to Department of
684 Biotechnology (DBT), Govt. of India for the award of Ramalingaswami re-entry fellowship
685 and Grant (No. BT/PR23666/AGIII/103/1039/2018) that supported this research. The *phr1*
686 *phl1* double mutant seeds were a gracious gift from by Prof. Tzyy-Jen Chiou, Academia Sinica,
687 Taipei. A crucial part of our investigations would not be possible without the gracious gift of
688 CSN5i-3 from Dr. Eva Altmann, Novartis Institutes for BioMedical Research, Switzerland.
689 Many thanks to Dr. Divya Chandran (RCB) for help with transcriptomic data analysis of *csn*
690 mutants. Y.W. thanks DBT for providing the Young Investigator award to her for pursuing this
691 research. K.D.I. acknowledges DBT for providing fellowships and KIIT University his PhD
692 registrations. M.K. thanks UGC for his PhD fellowship. D.L. acknowledges the Indian Institute
693 of Science for start-up funds. All authors thanks Dr. Nripendra Singh and his team at Advanced

Technology Platform Centre (ATPC), Faridabad, India for constant support with sample fractionations.

## Author Contributions

Y.W. and S.B. conceived and designed the research. D.L. and G.S. generated transgenic line used here Y.W. and S.B. performed most of the experiments. Y.W., K.D.I, M.K., and S.P. conducted and analyzed gene/protein expression changes. Y.W. and S.B. wrote the manuscript.

## Competing interests

The authors declare no conflict of interest for this study.

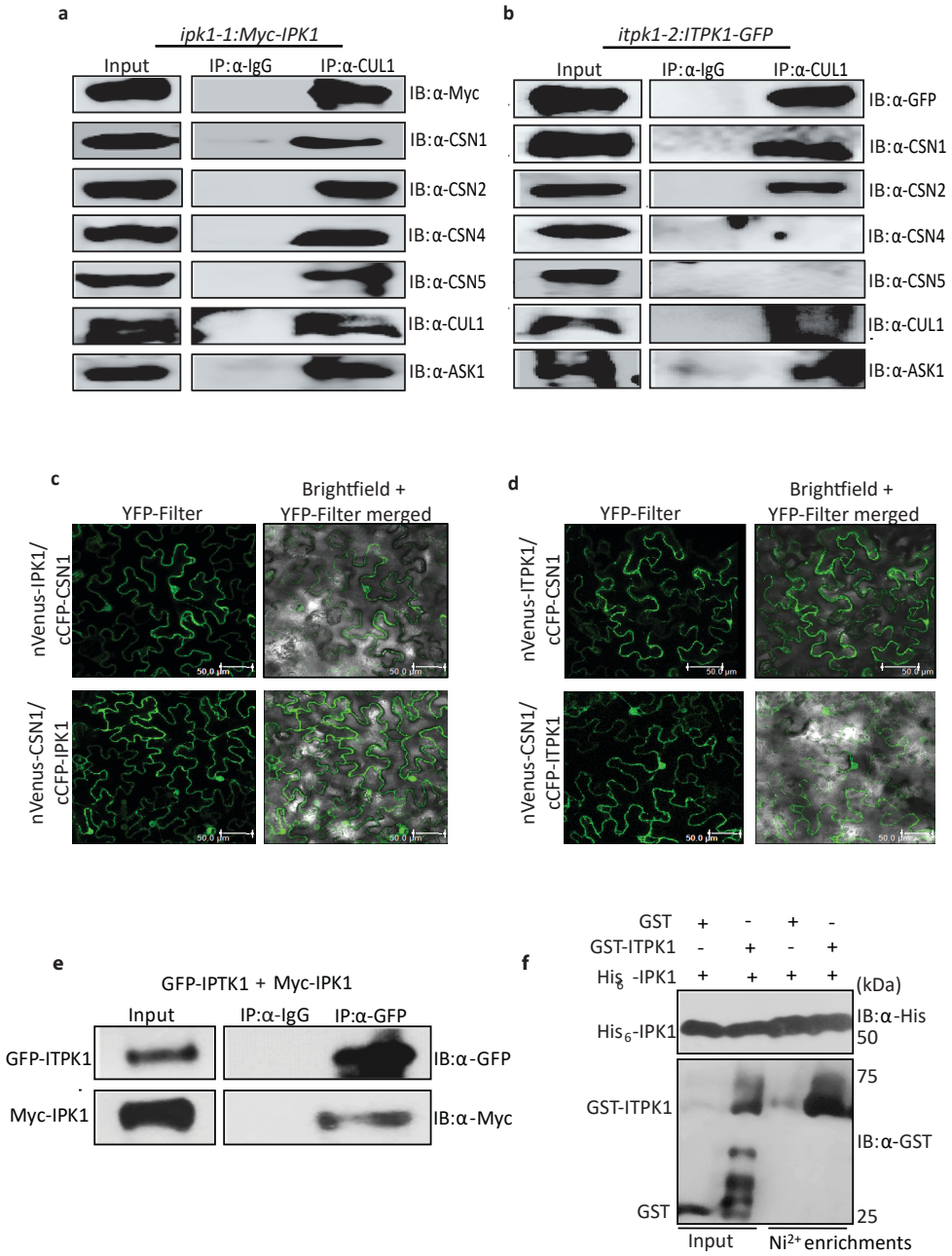


**Fig. 1. IPK1 and ITPK1 interact with each other and with selective CSN or CRLs components *in planta*. a-b,** Immuno-enrichments of IPK1 **(a)** or ITPK1 **(b)** from corresponding complemented lines (*ipk1-1: Myc-IPK1* or *itpk1-2:ITPK1-GFP*, respectively) and probed with anti-CSN1/2/4/5, anti-CUL1, or anti-ASK1 antibodies. IgG-agarose enrichments were used as negative controls. **c-d,** Bimolecular Fluorescence Complementation (BiFC) assays showing reciprocal combinations of **(c)** IPK1 and **(d)** ITPK1 interact with CSN1. Scale bar=50 µm. **e,** Co-immunoprecipitation of transiently expressed GFP-ITPK1 with Myc-IPK1. Immuno-enrichment was performed with anti-GFP antibody-conjugated agarose and probed with anti-GFP or anti-Myc antibodies. **f,** *In vitro* interactions of IPK1 with ITPK1. $His_6$-IPK1 was co-expressed with GST alone or GST-ITPK1 in *E. coli* cells. $Ni^{2+}$NTA-affinity enrichments were probed for $His_6$-IPK1 or GST-ITPK1 with anti-His or anti-GST antibodies, respectively. Migration positions of molecular weight markers (in kDa) and of $His_6$-IPK1, GST or GST-ITPK1 are shown on the right or left of each panel, respectively.

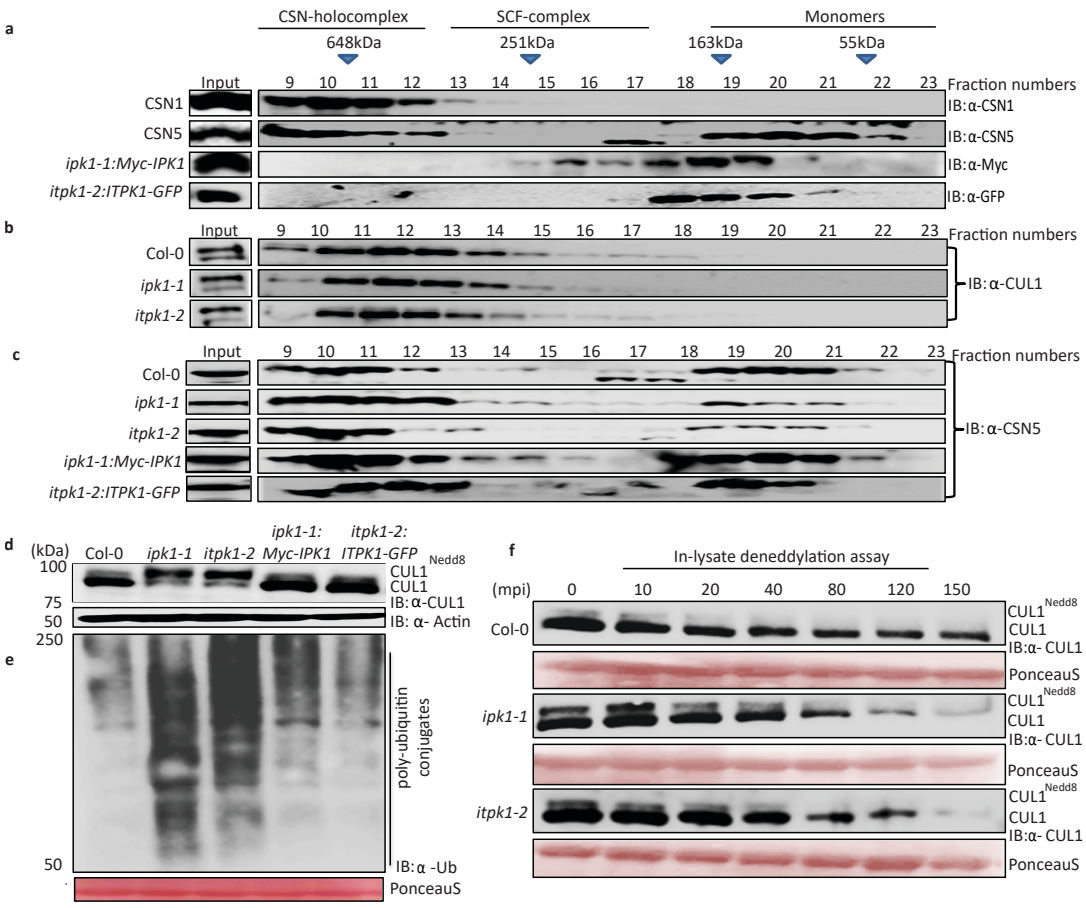


**Fig. 2. CSN5 partitioning and deneddylase functions are affected in *ipk1-1* or *itpk1-2*. a,** IPK1 or ITPK1 does not co-elute with the CSN holo-complex. **b,** CRL1 fractionation profiles are unchanged between Col-0, *ipk1-1* and *itpk1-2*. **c,** Enhanced CSN5 engagement on CSN holo-complex fractions in *ipk1-1* and *itpk1-2*. For fractionations, extracts were separated by size-exclusion chromatography and immuno-blotted with indicated antibodies. Right panels are immunoblots on input extracts. Fraction numbers are indicated above each lane. Numbers above arrowheads denote elution positions of molecular weight standards (in kDa). **d,** Increased neddylated CUL1 in *ipk1-1* or *itpk1-2*. **e,** Global polyubiquitin-conjugates are enhanced in *ipk1-1* or *itpk1-2*. For **d-e**, Total protein extracts were probed with anti-CUL1, anti-actin, or anti-Ubiquitin antibodies as indicated. **f,** CSN5-deneddylation deficiencies and lower CUL1 half-life in *ipk1-1* or *itpk1-2*. For in-lysate deneddylation assay total protein extracts incubated for indicated times (minutes post-incubation; mpi) were probed with anti-CUL1 antibodies. Migration position of molecular weight standards (in kDa) and neddylated ($CUL1^{Nedd8}$) or unneddylated (CUL1) cullin1 are shown. Anti-actin or Ponceau S staining demonstrate loadings controls.

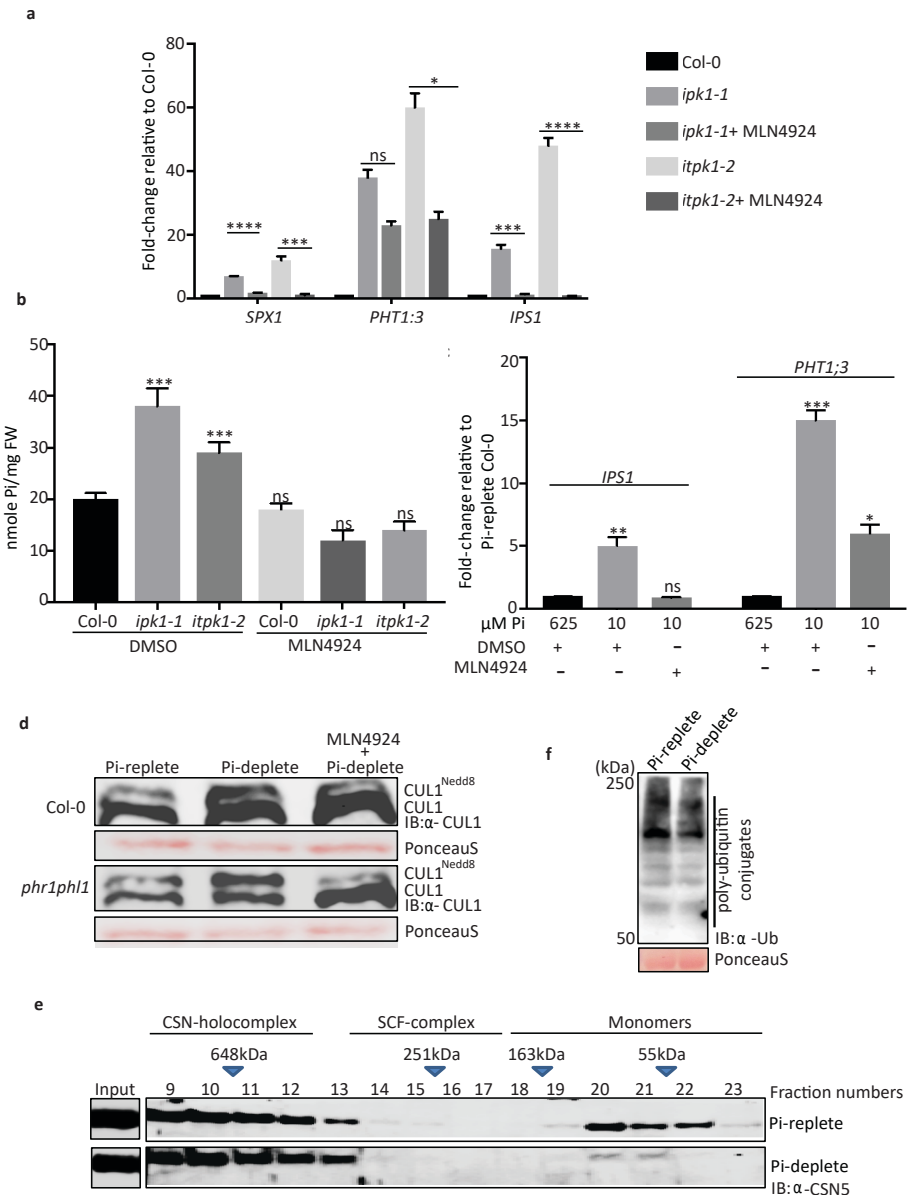


**Fig. 3. CUL1 deneddylation rates are reduced during Pi-starvation.** MLN4924 suppresses **a,** elevated PSI-gene expressions, and **b,** reduces endogenous Pi-levels in *ipk1-1* or *itpk1-2*. **c,** MLN4924 suppresses the induction of *PHT1;3* or *IPS1* expressions in Col-0 upon Pi-starvation. **d,** Enhanced CUL1-neddylation during Pi-deprivation is PHR1/PHL1-independent. **e,** Increased CSN5 partitioning on CSN holo-complex occur upon Pi-starvation. **f,** Global levels of polyubiquitin-conjugates are unperturbed during PSR. Gene expression changes were relative to *MON1* transcripts and reported as fold-change relative to Col-0 levels. Data is presented as mean ± SD (n=3 biological replicates of 3 plants in each). For Pi-estimation assays, data shown as mean ± SD (n= 6-7 plants). Asterisks denote significant differences from the reference sample. (Student's *t*-test; **P*<0.05, ***P* < 0.01; ****P* < 0.001, ****P*<0.0001. ns is not significant). For immunoblots, total protein extracts or fractions were probed with anti-CUL1 or anti-CSN5 or anti-ubiquitin antibodies, as indicated. Ponceau S staining show loadings controls. For Pi-deprivation/MLN4924 treatment assays, Seedlings grown in Pi-replete (625µM Pi) medium were either maintained or transferred to Pi-deplete (10 µM Pi) medium for three additional days in the presence of MLN4294 or absence (DMSO) during the shift, before being analyzed. Positions of molecular weight markers (in kDa) are shown.

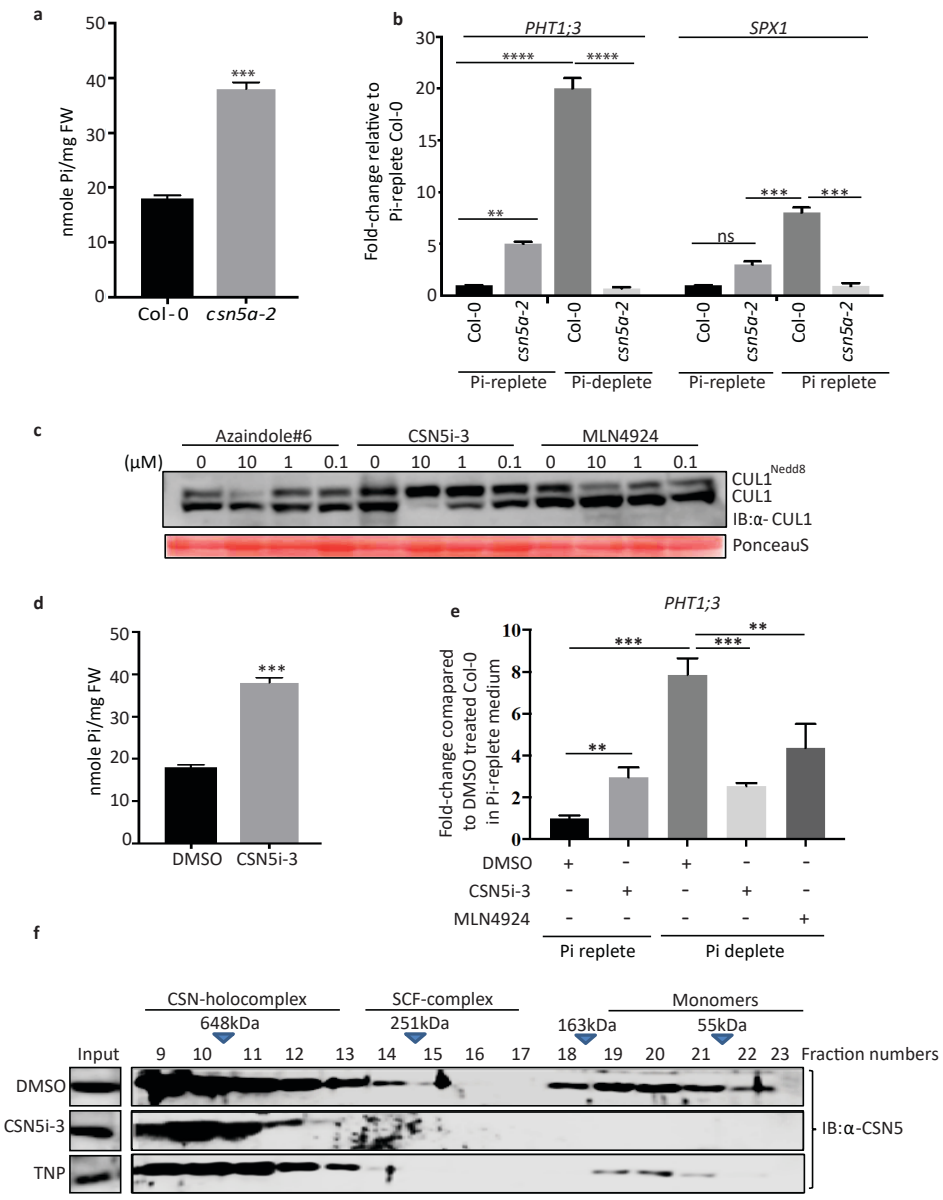


**Fig. 4. The dynamics of CSN5 is essential for responding to phosphate-starvation. a,** *csn5a-2* plants have elevated endogenous Pi levels. **b,** *csn5a-2* plants are deficient in inducing PSI-genes during Pi-starvation. **c,** CSN5i-3 shows dose-dependent inhibition in CUL1 deneddylation. Total protein extracts from Col-0, 24hrs post-treated with indicated doses of the inhibitors mentioned, were probed with anti-CUL1 antibodies. Ponceau S staining shows loading controls. **d,** CSN5i-3 treatment elevates endogenous Pi-levels. **e,** CSN5i-3 suppresses *PHT1;3* induction in Col-0 during phosphate-starvation. **f,** CSN5 is enriched in CSN holo-complex pools upon CSN5i-3 or TNP treatment. Fractionation was performed 24hrs post-inhibitor treatment and fractions immunoblotted with anti-CSN5 antibodies. For Pi-estimation assays, error bars show SD from mean (n=3 replicates of 5-6 plants each). For gene expression changes, *MON1* levels were used as internal controls and results reported as fold-change relative to untreated Pi-replete grown Col-0. Data is mean ± SD (n=3 replicates, 3-4 plants each). Statistical significance was calculated with Student's *t*-test and depicted with $*P<0.05$, $**P<0.01$; $***P<0.001$, $***P<0.0001$. ns is not significant. For Pi-deprivation assays, plants grown in Pi-replete (625μM Pi) media were transferred for 3 days to Pi-deplete (10 μM Pi) media with or without indicated inhibitors before analysis.

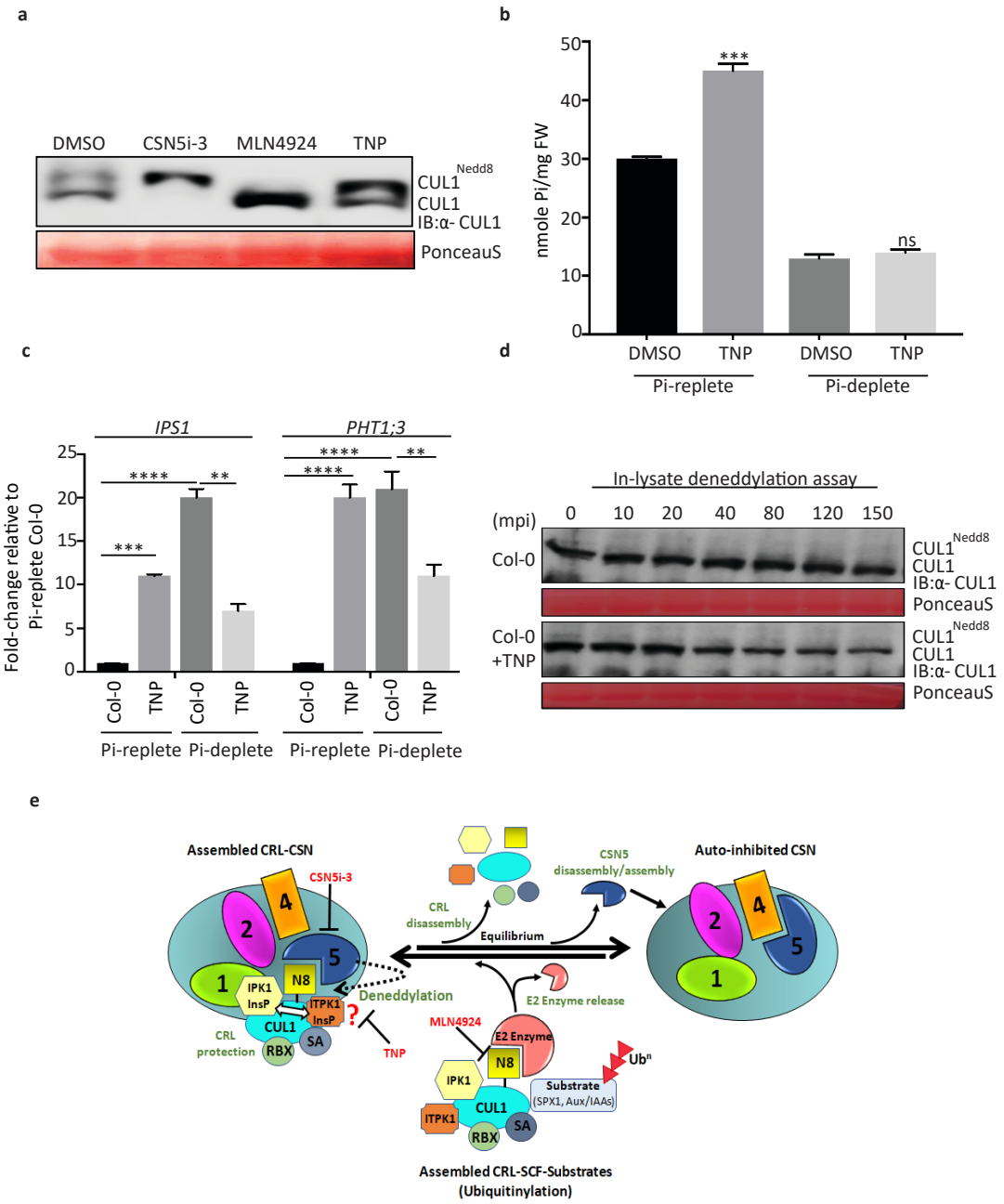


**Fig. 5. ITPK1 activity regulates CSN5 dynamics and deneddylase functions. a,** TNP treatment enhances pools of neddylated CUL1. Total protein extracts from Col-0 at 24hrs post-inhibitor treatment were immunoblotted with anti-CUL1 antibodies. **b,** TNP treatments increase endogenous Pi-content in Col-0. Error bars are mean ± SD (n=3 replicates of 5-6 plants each). **c,** TNP suppresses *IPS1* or *SPX1* in Col-0 upon Pi-starvation. For Pi-starvation, plants grown in Pi-replete medium were transferred for 3 days to Pi-deplete medium with or without TNP. Expression levels of *MON1* transcripts was used as internal reference. Error bars denote mean with SD (n=3 biological replicates of 3-4 plants each). Student's *t*-test was used to calculate statistical significance and shown as $^{**}P<0.01$, $^{***}P<0.001$, $^{****}P<0.0001$, ns not significant. **d,** TNP reduces CUL1 deneddylation and increases CUL1 instability. In-lysate deneddylation assay on Col-0 extracts post-24hrs TNP-treatment and then probed with anti-

782 CUL1 antibodies. Ponceau S staining indicates loadings control. **e,** Schematic representation
783 of IPK1-ITPK1 role on CRL-CSN association/dissociation equilibrium in plants. CSN holo-
784 complex platform offers protection to CRLs in absence of ubiquitinylation substrates (E2
785 enzyme prevented from binding due to mutual exclusion[43,44]) utilizing coordinated locale-
786 specific activities (bi-directional white arrows) of IPK1 and ITPK1. Stimulus/energy status-
787 dependent modulation in localized IPK1/ITPK1 activities (InsPs nature unknown; red question
788 mark) is coupled to CRL, CSN5 disassembly and CUL1 deneddylation. Auto-inhibited CSN
789 holo-complex is reconstituted by re-incorporating CSN5. Active CRL-SCF complex binds E2
790 ubiquitin enzyme to cause targeted ubiquitinylation ($Ub^n$) and degradation of substrates (such
791 as SPX1 or Aux/IAA repressors). Inhibitory functions of TNP, CSN5i-3 and MLN4924 are
792 indicated on the respective processes. CSN subunits are presented as numbers; CUL1, Cullin1;
793 RBX, RING H2 protein1; SA, substrate adapter, N8, Nedd8, IPK1, inactive IPK1, ITPK1,
794 inactive ITPK1, IPK1 InsP, active IPK1, ITPK1 InsP, active ITPK1.

795 **Extended Data Figure legends.**

796 **Extended Data Fig. 1. Complemented lines restore PSR defects of *ipk1-1* and *itpk1-2*. a,**
797 Endogenous Pi levels in Col-0, *ipk1-1*, *itpk1-2* and respective complemented lines *ipk1-1:Myc-*
798 *IPK1* or *itpk1-2:ITPK1-GFP*. Data is represented as mean with SD (n=3 replicates of 3-4 plants
799 each). **b,** Relative expression levels of *SPX1* in the indicated plants. Transcript levels were
800 normalized to internal standard *MON1* expressions and are reported as fold-change relative to
801 Col-0. Error bars indicate SD (n=3, three replicates of 3 plants each). Statistical significance
802 was calculated by Student's *t*-test and reported with asterisks **P*<0.05, ***P* < 0.01; ****P* <
803 0.001, ****P*<0.0001. ns is not significant.

804 **Extended Data Fig. 2. *In planta* interactions between IPK1, ITPK1 and CSN2.** BiFC assays
805 showing interactions of **a,** IPK1 with CSN2. **b,** ITPK1 with CSN2. **c,** IPK1 with ITPK1. **d,**
806 Lack of interactions between the negative control GUS with IPK1, ITPK1, CSN1 or CSN2 is
807 shown. Agrobacterium strains expressing the indicated BiFC vectors (mentioned on the left of
808 each panel) were co-infiltrated in *N. benthamiana* leaves. Infiltrated leaf areas were visualized
809 at 48 hpi (hours post-infiltration) under a confocal microscope and imaged with YFP and bright
810 field filters. Figures are representative of multiple images obtained for each BiFC
811 combinations. Scale bar=50μM.

812 **Extended Data Fig. 3. CSN4 fractionation profiles are not affected in *ipk1-1* or *itpk1-2*.**
813 Total protein extracts from indicated plants were separated by size-exclusion chromatography
814 and immuno-blotted with anti-CSN4 antibodies. Right panels show detection of CSN4 in input
815 extracts. Fraction numbers are marked. Numbers above the arrowheads denote the elution
816 positions of molecular weight standards (in kDa). Fractions corresponding to CSN holo-
817 complex, SCF-complex, and CSN4 monomers are indicated.

818 **Extended Data Fig. 4. CRL-CSN associations are not affected in *ipk1-1* or *itpk1-2*. a,**
819 Immuno-enrichment of CUL1 detects stoichiometrically similar amounts of CSN1 and CSN2
820 in *ipk1-1* or *itpk1-2* to Col-0. Total protein extracts were immunoprecipitated with either IgG
821 or anti-CUL1 antibodies and immunoblotted with anti-CUL1, anti-CSN1 or anti-CSN2
822 antibodies. Western blots on input extracts are shown on the left panels. Migration position of
823 molecular weight markers (in kDa) are indicated.

824 **Extended Data Fig. 5. Global levels of neddylated CUL1 are not enhanced in *vih2-4* or**
825 ***ipk2β-1* plants.** Total protein extracts from indicated plants was immunoblotted with anti-
826 CUL1 antibodies. Migration position of neddylated: unneddylated CUL1 ($CUL1^{Nedd8}$:CUL1)
827 are shown. Ponceau S stained membrane demonstrates equal loading controls.

828 **Extended Data Fig. 6. Pi-starvation does aggravate increased neddylated CUL1 in *ipk1-1***
829 **or *itpk1-2*.** Total protein extracts from indicated plants grown in Pi-replete (625μM Pi) medium
830 and then transferred for 3-days to Pi-deplete (10μM Pi) medium, were immunoblotted with
831 anti-CUL1 antibodies. Relative positions of $CUL1^{Nedd8}$:CUL1 are shown. Anti-actin
832 immunoblot shows comparable protein loadings.

833 **Extended Data Fig. 7. CUL1 deneddylation efficiencies but not stability is reduced upon**
834 **Pi-starvation.** In-lysate deneddylation assay was performed on total protein extracts from 14-
835 day-old Col-0 plants Pi-starved (10μM Pi) or Pi-sufficient (625μM Pi) for the last 3-days.
836 Extracts were incubated for the indicated times (minutes post-incubation, mpi) and immuno-
837 blotted with anti-CUL1 antibodies. Relative migration positions of $CUL1^{Nedd8}$:CUL1 are
838 shown. Ponceau S staining shows equal protein loadings.

839 **Extended Data Fig. 8. Pi-starvation does not alter CSN1 or CUL1 fractionation profiles**
840 **a,** CSN1 and CUL1 profiles under Pi-replete and Pi-deplete conditions. Size-exclusion
841 fractionation of total protein extracts from Col-0 grown for a total period of 14-days with the

842 last 3 days either in Pi-replete (625μM Pi) or Pi-deplete (10μM Pi) medium. Fractions were
843 immunoblotted with anti-CSN1 or anti-CUL1 antibodies. Fraction numbers and elution
844 positions of molecular weight standards are indicated. Fractions corresponding to CSN holo-
845 complex, SCF-complex and lower molecular weight pools are marked. **b,** Enhanced
846 accumulation of IPK1 and ITPK1 under Pi-deplete conditions. Total extracts prepared from
847 indicated plants with treatments as above and probed with anti-Myc or anti-GFP antibodies.
848 Ponceau S staining for Rubisco shows loadings controls.

849 **Extended Data Fig. 9.** The differential expression of PSI-genes in *csn* mutants with respect to
850 wild-type (Wt) are extracted from the microarray data reported in Dohmann et al (2008)[36]. The
851 heatmap is generated using Graphpad Prism 8.4.3 using double gradient Heatmap function.
852 The expression change is shown as $\log_2$FC(Fold-Change) values of different genes with Green
853 for downregulated genes, Red for upregulated genes and black for either genes which show no
854 change or the genes with expression values which are not significant (Adjusted $P > 0.10$).

855 **Extended Data Fig. 10. CSN5i-3 inhibits CUL1 deneddylation in Col-0 in dose-dependent**
856 **increments.** 14-day-old Col-0 plants were treated with indicated doses (in μM) of
857 Azaindole#6, CSN5i-3 or MLN4924 for 48hrs. Total proteins extracts were immunoblotted
858 with anti-CUL1 antibodies. Positions of neddylated ($CUL1^{Nedd8}$) and unneddylated CUL1 is
859 shown. Ponceau S staining shows comparable loading across samples.

860 **Extended Data Fig. 11.** CSN5 inhibitions suppresses induction of PSI-genes. **a,** CSN5i-3
861 suppresses *SPX1* induction in Col-0 during phosphate-starvation. **b,** Upregulated *IPS1*
862 expressions in *ipk1-1* or *itpk1-2* is suppressed in the presence of CSN5i-3. Gene expression
863 changes are relative to *MON1* levels. Data reported is mean ± SD (n=3 replicates, 3-4 plants
864 each). Statistical significance is according to Student's *t*-test and shown as $*P<0.05$, $**P< 0.01$;
865 $***P< 0.001$, $****P<0.0001$. ns is not significant. Pi-deprivation assays involved transfer of

866 Pi-replete (625μM Pi) grown plants to Pi-deplete (10μM Pi) medium with or without inhibitors
867 for 3 days before being analyzed.

868 **Extended Data Fig. 12. Supplemented $InsP_6$ does not affect CUL1 deneddylation rate or**
869 **stability. a,** In-lysate deneddylation assay on total protein extracts isolated from Col-0, *ipk1-*
870 *1*, or *itpk1-2* plants. Extracts were supplemented with or without 0.2μM $InsP_6$, incubated for
871 indicated times (minutes post-incubation; mpi) and probed with anti-CUL1 antibodies. **b,**
872 CUL1 neddylations remain comparable to Col-0 in *itpk4-1*. Total protein extracts were
873 immunoblotted with anti-CUL1 antibodies. Relative migrations of neddylated:unneddylated
874 CUL1 ($CUL1^{Nedd8}$:CUL1) are indicted. Loading controls are shown by Ponceau S staining.

875 **Supplementary Table 1.** List of oligonucleotide primers used in this study.

876

877

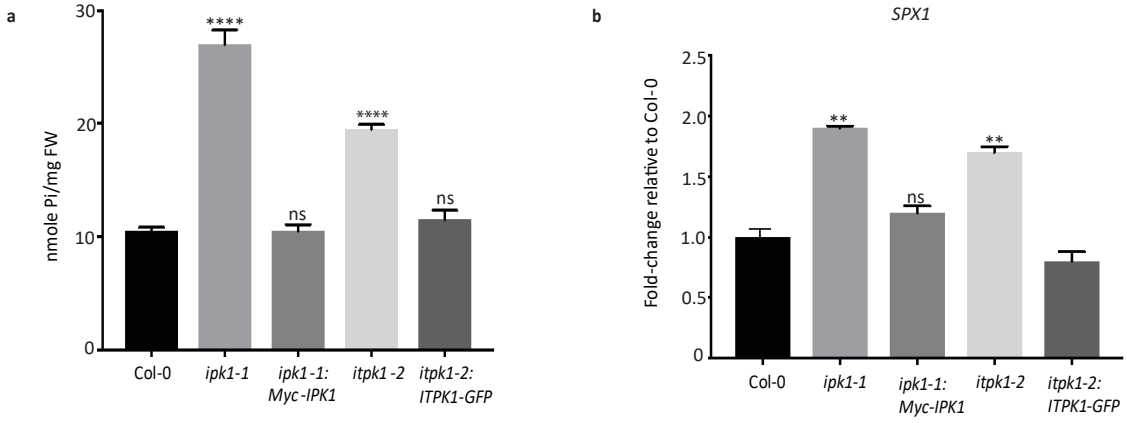


878

879 **Extended Data Fig. 1. Complemented lines restore PSR defects of *ipk1-1* and *itpk1-2*. a,**
880 Endogenous Pi levels in Col-0, *ipk1-1*, *itpk1-2* and respective complemented lines *ipk1-1:Myc-*
881 *IPK1* or *itpk1-2:ITPK1-GFP*. Data is represented as mean with SD (n=3 replicates of 3-4 plants
882 each). **b,** Relative expression levels of *SPX1* in the indicated plants. Transcript levels were
883 normalized to internal standard *MON1* expressions and are reported as fold-change relative to
884 Col-0. Error bars indicate SD (n=3, three replicates of 3 plants each). Statistical significance
885 was calculated by Student's *t*-test and reported with asterisks **P*<0.05, ***P* < 0.01; ****P* <
886 0.001, ****P*<0.0001. ns is not significant.

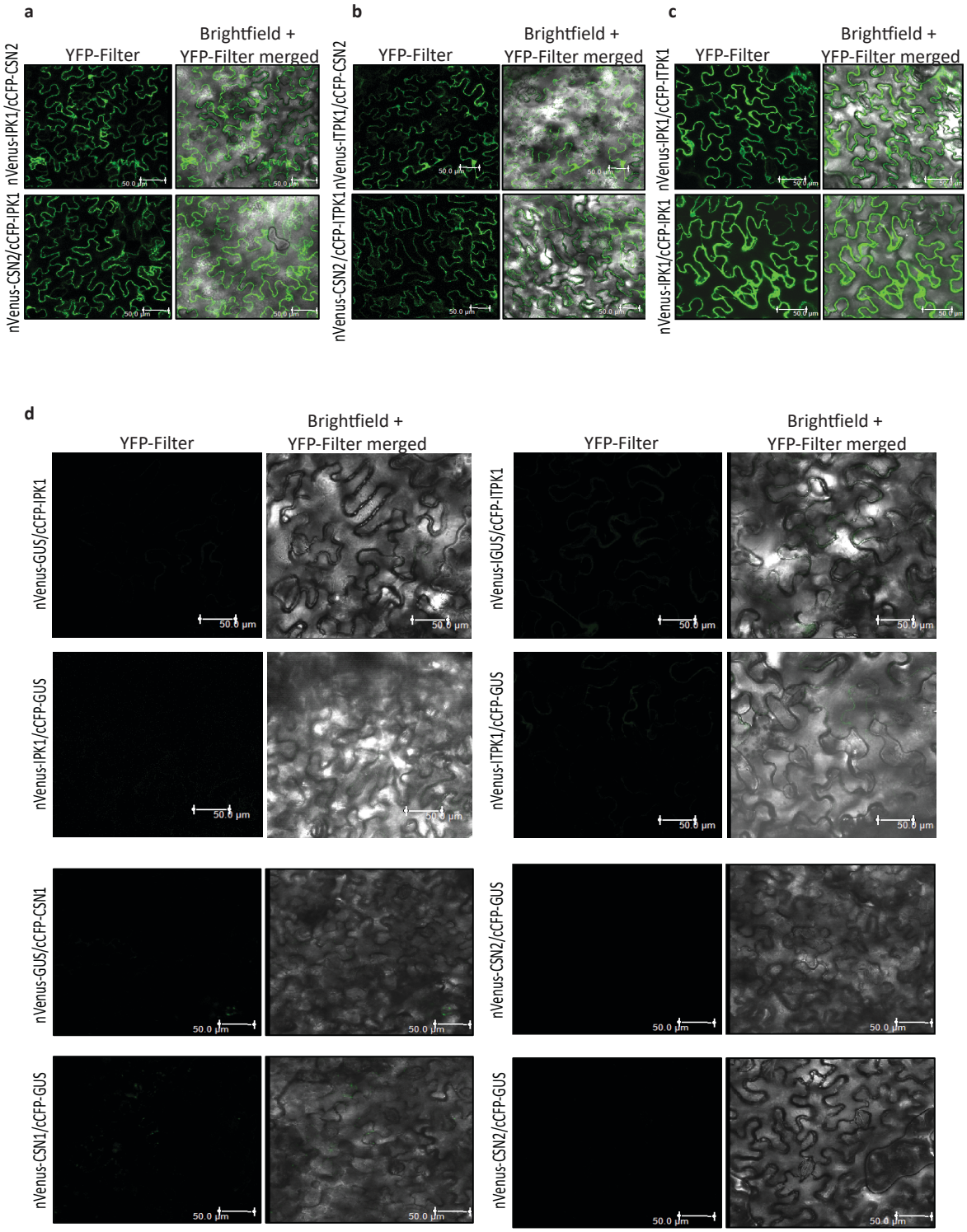


**Extended Data Fig. 2. *In planta* interactions between IPK1, ITPK1 and CSN2.** BiFC assays showing interactions of **a,** IPK1 with CSN2. **b,** ITPK1 with CSN2. **c,** IPK1 with ITPK1. **d,** Lack of interactions between the negative control GUS with IPK1, ITPK1, CSN1 or CSN2 is shown. Agrobacterium strains expressing the indicated BiFC vectors (mentioned on the left of each panel) were co-infiltrated in *N. benthamiana* leaves. Infiltrated leaf areas were visualized at 48 hpi (hours post-infiltration) under a confocal microscope and imaged with YFP and bright field filters. Figures are representative of multiple images obtained for each BiFC combinations. Scale bar =50µM.

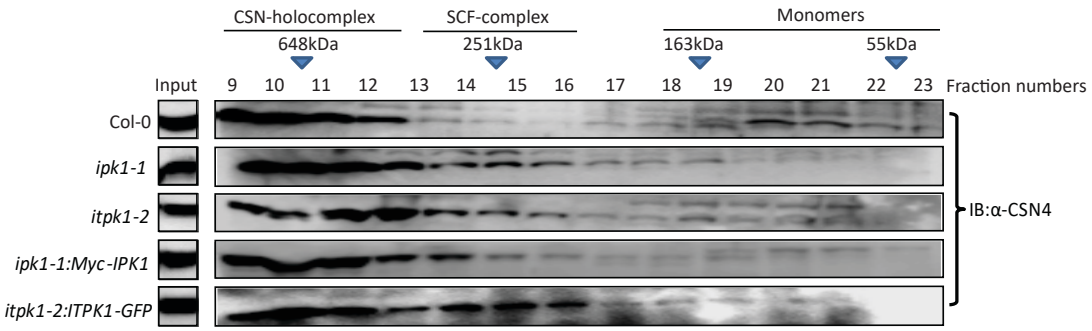


**Extended Data Fig. 3. CSN4 fractionation profiles are not affected in *ipk1-1* or *itpk1-2*.** Total protein extracts from indicated plants were separated by size-exclusion chromatography and immuno-blotted with anti-CSN4 antibodies. Right panels show detection of CSN4 in input extracts. Fraction numbers are marked. Numbers above the arrowheads denote the elution positions of molecular weight standards (in kDa). Fractions corresponding to CSN holo-complex, SCF-complex, and CSN4 monomers are indicated.

903

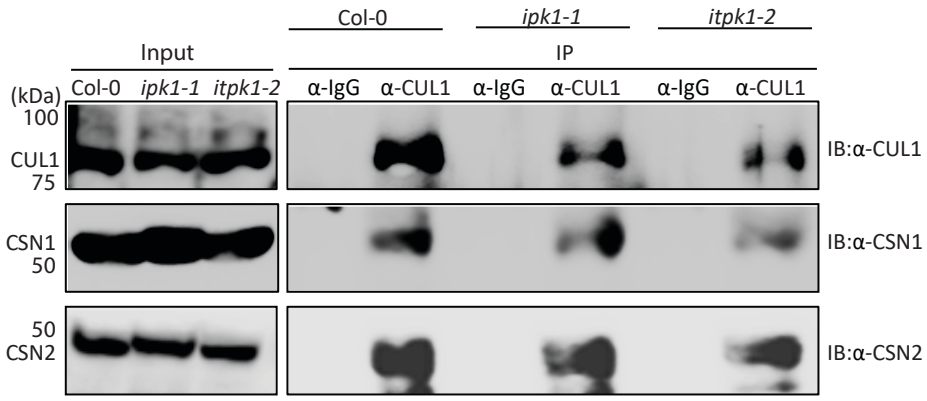


904

905 **Extended Data Fig. 4. CRL-CSN associations are not affected in *ipk1-1* or *itpk1-2*. a,**
906 Immuno-enrichment of CUL1 detects stoichiometrically similar amounts of CSN1 and CSN2
907 in *ipk1-1* or *itpk1-2* to Col-0. Total protein extracts were immunoprecipitated with either IgG
908 or anti-CUL1 antibodies and immunoblotted with anti-CUL1, anti-CSN1 or anti-CSN2
909 antibodies. Western blots on input extracts are shown on the left panels. Migration position of
910 molecular weight markers (in kDa) are indicated.

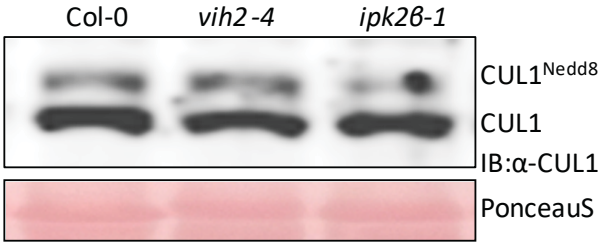


**Extended Data Fig. 5. Global levels of neddylated CUL1 are not enhanced in *vih2-4* or *ipk2β-1* plants.** Total protein extracts from indicated plants was immunoblotted with anti-CUL1 antibodies. Migration position of neddylated: unneddylated CUL1 ($CUL1^{Nedd8}$:CUL1) are shown. Ponceau S stained membrane demonstrates equal loading controls.

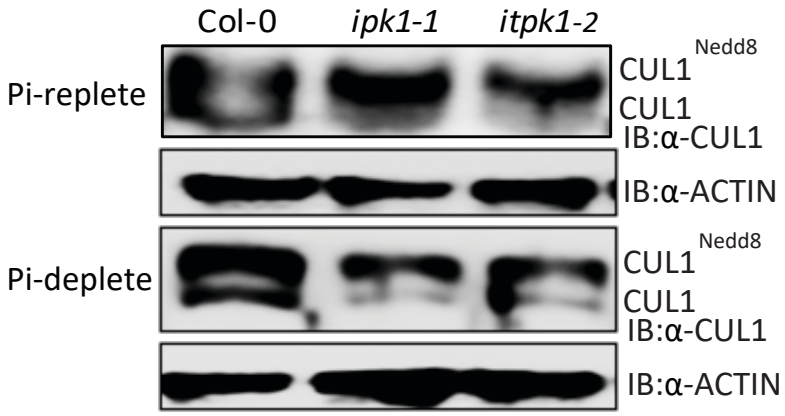


**Extended Data Fig. 6. Pi-starvation does aggravate increased neddylated CUL1 in *ipk1-1* or *itpk1-2*.** Total protein extracts from indicated plants grown in Pi-replete (625μM Pi) medium and then transferred for 3-days to Pi-deplete (10μM Pi) medium, were immunoblotted with anti-CUL1 antibodies. Relative positions of $CUL1^{Nedd8}$:CUL1 are shown. Anti-actin immunoblot shows comparable protein loadings.

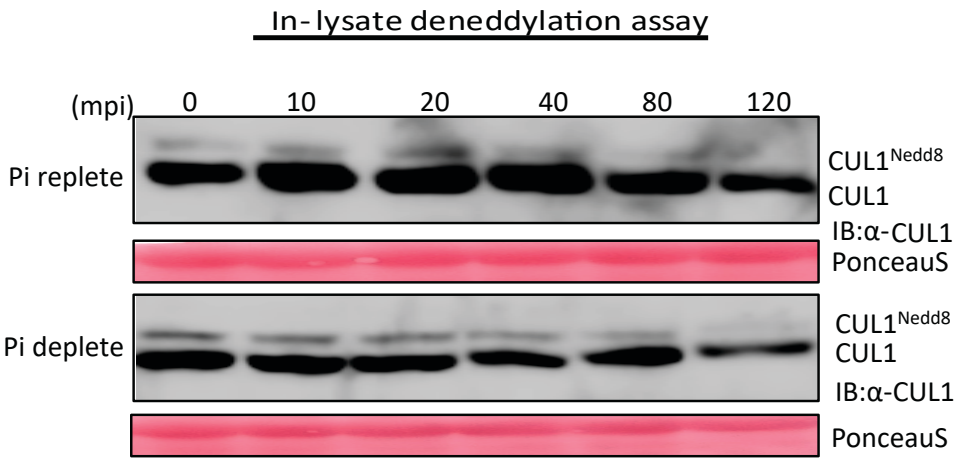


**Extended Data Fig. 7. CUL1 deneddylation efficiencies but not stability is reduced upon Pi-starvation.** In-lysate deneddylation assay was performed on total protein extracts from 14-day-old Col-0 plants Pi-starved (10µM Pi) or Pi-sufficient (625µM Pi) for the last 3-days. Extracts were incubated for the indicated times (minutes post-incubation, mpi) and immuno-blotted with anti-CUL1 antibodies. Relative migration positions of $CUL1^{Nedd8}$:CUL1 are shown. Ponceau S staining shows equal protein loadings.

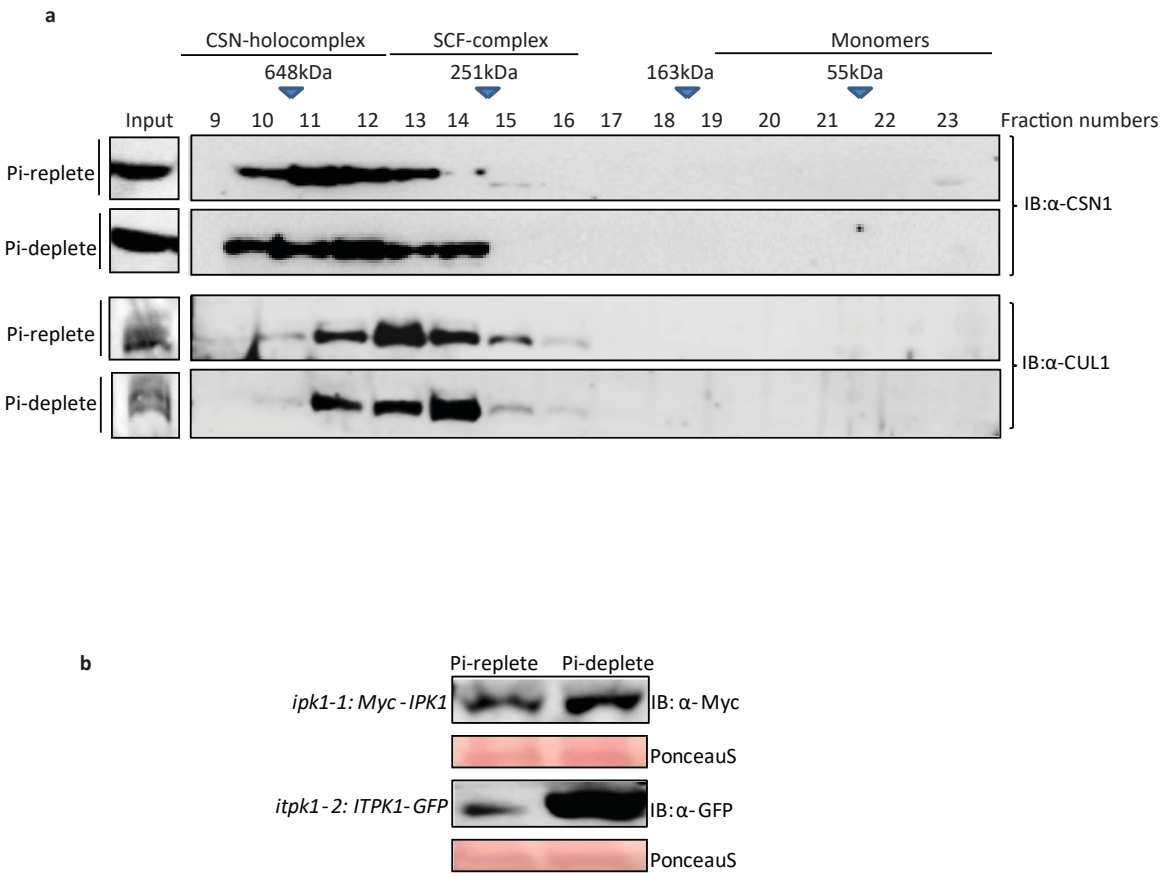


934

935

936 **Extended Data Fig. 8. Pi-starvation does not alter CSN1 or CUL1 fractionation profiles**
937 **a,** CSN1 and CUL1 profiles under Pi-replete and Pi-deplete conditions. Size-exclusion
938 fractionation of total protein extracts from Col-0 grown for a total period of 14-days with the
939 last 3 days either in Pi-replete (625µM Pi) or Pi-deplete (10µM Pi) medium. Fractions were
940 immunoblotted with anti-CSN1 or anti-CUL1 antibodies. Fraction numbers and elution
941 positions of molecular weight standards are indicated. Fractions corresponding to CSN holo-
942 complex, SCF-complex and lower molecular weight pools are marked. **b,** Enhanced
943 accumulation of IPK1 and ITPK1 under Pi-deplete conditions. Total extracts prepared from
944 indicated plants with treatments as above and probed with anti-Myc or anti-GFP antibodies.
945 Ponceau S staining for Rubisco shows loadings controls.

946

947

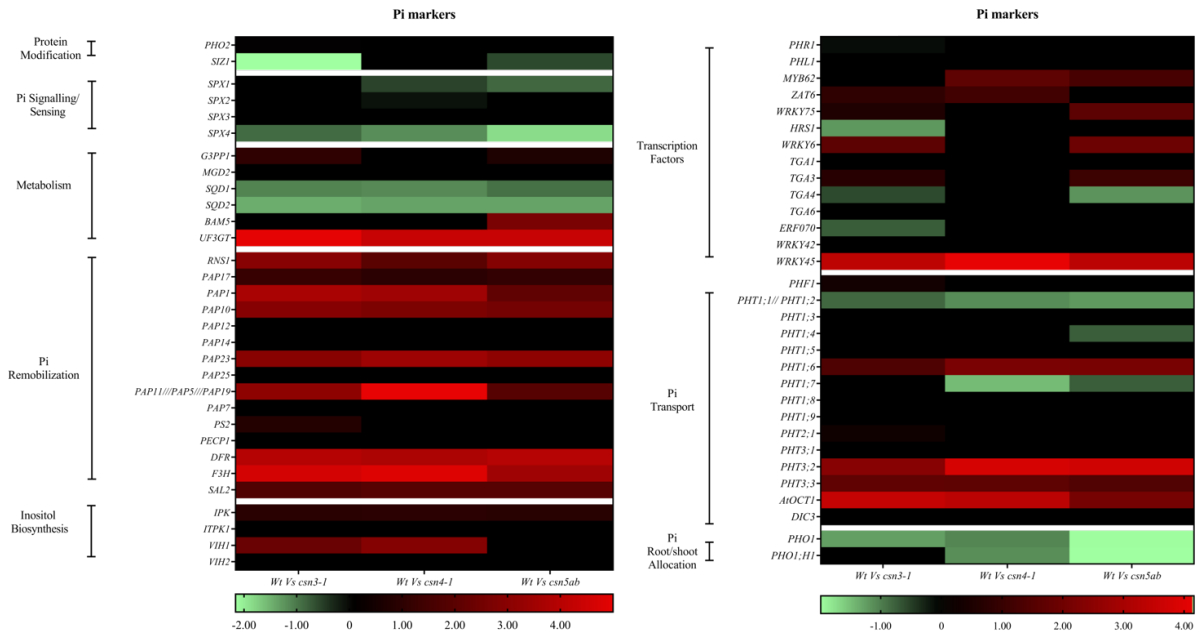


**Extended Data Fig. 9.** The differential expression of PSI-genes in *csn* mutants with respect to wild-type (Wt) are extracted from the microarray data reported in Dohmann et al (2008)[36]. The heatmap is generated using Graphpad Prism 8.4.3 using double gradient Heatmap function. The expression change is shown as $\log_2$FC(Fold-Change) values of different genes with Green for downregulated genes, Red for upregulated genes and black for either genes which show no change or the genes with expression values which are not significant (Adjusted $P > 0.10$).

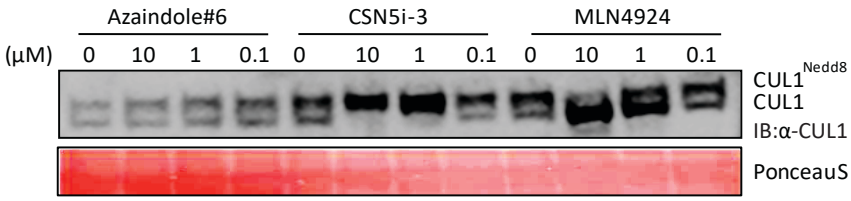


957

958 **Extended Data Fig. 10. CSN5i-3 inhibits CUL1 deneddylation in Col-0 in dose-dependent**
959 **increments.** 14-day-old Col-0 plants were treated with indicated doses (in μM) of
960 Azaindole#6, CSN5i-3 or MLN4924 for 48hrs. Total proteins extracts were immunoblotted
961 with anti-CUL1 antibodies. Positions of neddylated ($CUL1^{Nedd8}$) and unneddylated CUL1 is
962 shown. Ponceau S staining shows comparable loading across samples.

963

964

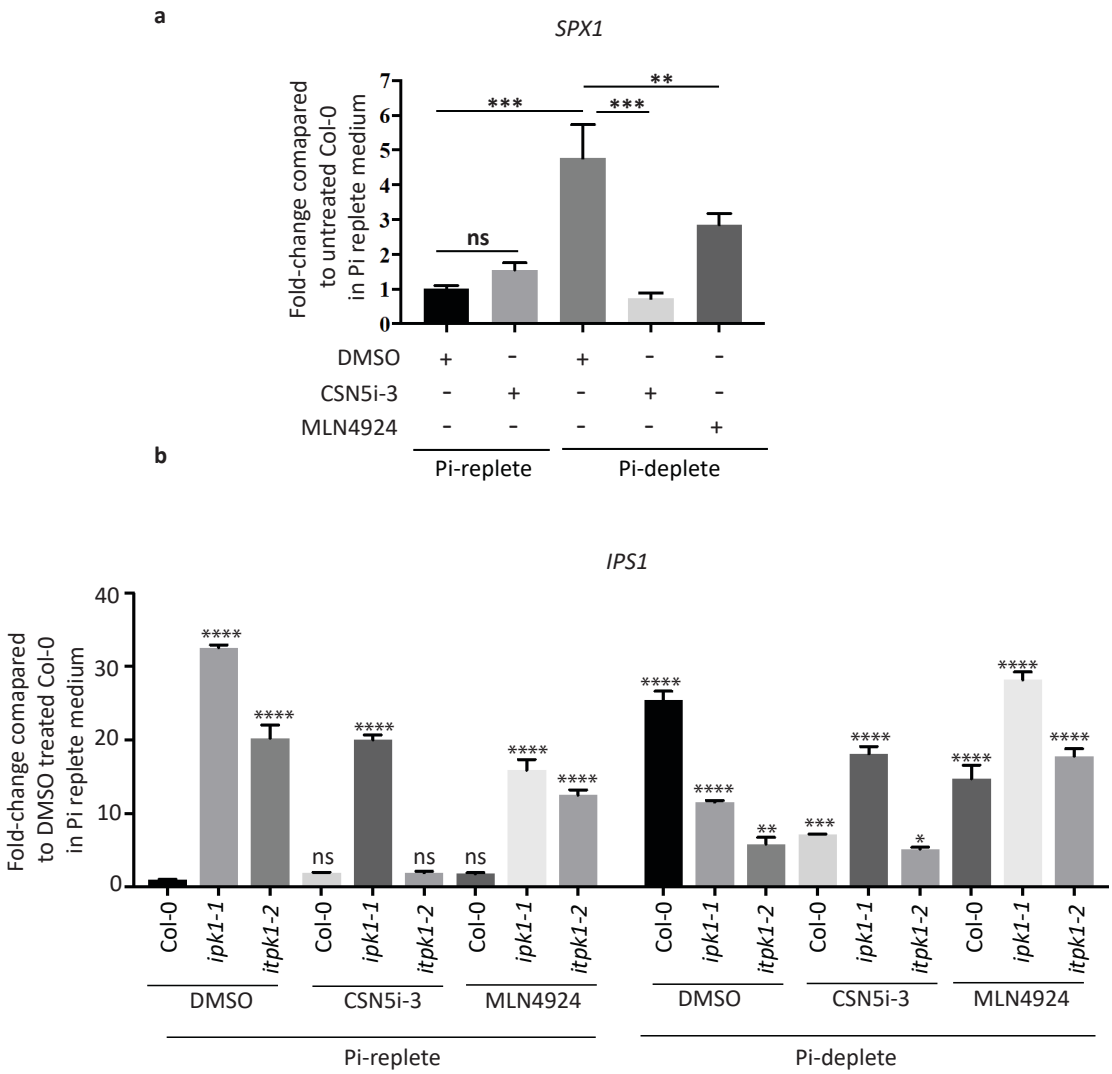


**Extended Data Fig. 11. CSN5 inhibitions suppresses induction of PSI-genes**. **a,** CSN5i-3 suppresses *SPX1* induction in Col-0 during phosphate-starvation. **b,** Upregulated *IPS1* expressions in *ipk1-1* or *itpk1-2* is suppressed in the presence of CSN5i-3. Gene expression changes are relative to *MON1* levels. Data reported is mean ± SD (n=3 replicates, 3-4 plants each). Statistical significance is according to Student's *t*-test and shown as **P*<0.05, ***P*< 0.01; ****P*< 0.001, *****P*<0.0001. ns is not significant. Pi-deprivation assays involved transfer of Pi-replete (625µM Pi) grown plants to Pi-deplete (10µM Pi) medium with or without inhibitors for 3 days before being analyzed.

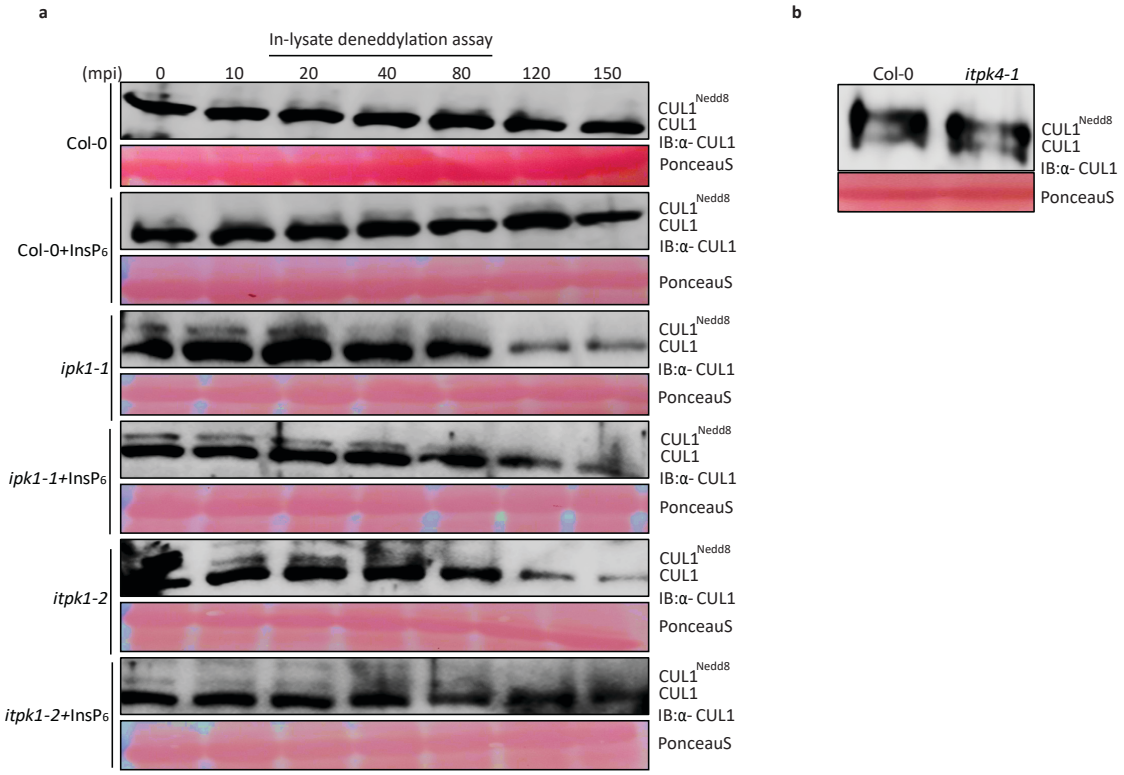


**Extended Data Fig. 12. Supplemented $InsP_6$ does not affect CUL1 deneddylation rate or stability. a,** In-lysate deneddylation assay on total protein extracts isolated from Col-0, *ipk1-1*, or *itpk1-2* plants. Extracts were supplemented with or without 0.2μM $InsP_6$, incubated for indicated times (minutes post-incubation; mpi) and probed with anti-CUL1 antibodies. **b,** CUL1 neddylations remain comparable to Col-0 in *itpk4-1*. Total protein extracts were immunoblotted with anti-CUL1 antibodies. Relative migrations of neddylated:unneddylated CUL1 ($CUL1^{Nedd8}$:CUL1) are indicted. Loading controls are shown by Ponceau S staining.

986 **Supplementary Table 1. Oligonucleotide primers used in this study.**

| S. No | Primer Name | Primer Sequence (5' to 3') | Purpose |
|---|---|---|---|
| 1. | attB1 *IPK1* For | GGGGACAAGTTTGTACAAAAAAGCAGGCTCAATGGAGATGATTTTGGAGG | Gateway cloning of IPK1 cDNA in pDONR207 |
| 2. | attB2 *IPK1* Rev | GGGGACCACTTTGTACAAGAAAGCTGGGTATTAGCTGTGGGAAGGTTTTGAG | Gateway cloning of IPK1 cDNA in pDONR207 |
| 3. | attB1 *ITPK1* For | GGGGACAAGTTTGTACAAAAAAGCAGGCTCAATGTCAGATTCAATCCAG | Gateway cloning of ITPK1 cDNA in pDONR207 |
| 4. | attB1 *ITPK1* Rev | GGGGACCACTTTGTACAAGAAAGCTGGGTATCAGACATGATTCTTCTTAGTG | Gateway cloning of ITPK1 cDNA in pDONR207 |
| 5. | attB1 *CSN1* For | GGGGACAAGTTTGTACAAAAAAGCAGGCTCA ATGGAGCGAGACGAAGAAGCGAGT | Gateway cloning of CSN1 cDNA in pDONR207 |
| 6. | attB2 *CSN1* Rev | GGGGACCACTTTGTACAAGAAAGCTGGGTATCAAAGTTTCCTTGCCGATCTGGCATG | Gateway cloning of CSN1 cDNA in pDONR207 |
| 7. | attB1 *CSN2* For | GGGGACAAGTTTGTACAAAAAAGCAGGCTCAATGGCTTCAGATGCTGACATGGAGGAC | Gateway cloning of CSN2 cDNA in pDONR207 |
| 8. | attB2 *CSN2* Rev | GGGGACCACTTTGTACAAGAAAGCTGGGTATTAACACAGTCGGCTGGTGATATTTGA | Gateway cloning of CSN2 cDNA in pDONR207 |
| 9. | qRT-PCR *PHT1;2* For | AGCCATCATTGGAGCCTTC | For qRT-PCRs |
| 10. | qRT-PCR *PHT1;2* Rev | ACCTTAGCCTTGTCTTGATT | For qRT-PCRs |
| 11. | qRT-PCR *IPS1* For | GCGTTTTAAGATATGGAGCAATG | For qRT-PCRs |

| | | | |
|---|---|---|---|
| 12. | qRT-PCR *IPS1* Rev | CGAAGCTTGCCAAAGGATAG | For qRT-PCRs |
| 13. | qRT-PCR *SPX1* For | GATTCCATTGTTGGAGCAAGA | For qRT-PCRs |
| 14. | qRT-PCR *SPX1* Rev | AATCTTGTTAGCTTCTTCTATTGTA | For qRT-PCRs |
| 15. | qRT-PCR *PHT1;3* For | AAACATTGTGAACCATGCTAACCCTT | For qRT-PCRs |
| 16. | qRT-PCR *PHT1;3* Rev | GATAAACAAAATTGATTGGAATGACCACTA | For qRT-PCRs |
| 17. | qRT-PCR MON1 For | AACTCTATGCAGCATTTGATCCACT | For qRT-PCRs |
| 18. | qRT-PCR *MON1* Rev | TGATTGCATATCTTTATCGCCATC | For qRT-PCRs |
| 19. | *ipk1-1* RP | TTTCAATCAAGGAATGCTTGG | Genotyping *ipk1-1* |
| 20. | *ipk1-1* LP | ATGCTACGGGAAACCATTTTC | Genotyping *ipk1-1* |
| 21. | *itpk1-2* RP | CCATGTCCCAGAAGAACTCAG | Genotyping *itpk1-2* |
| 22. | *itpk1-2* LP | ACCAATATTCGATTCGATTCCACACG | Genotyping *itpk1-2* |
| 23. | LB1.3 | ATTTTGCCGATTTCGGAAC | T-DNA Left-border primer (for *ipk1-1*) |
| 24. | LB3 | TAGCATCTGAATTTCATAACCAATCTCGATACAC | T-DNA Left-border primer (for *itpk1-2*) |
| 25. | AJHIFW2 | GTTTTGGATTAGCATTAGTCCCCAAATC | Genotyping *csn5a-2* plants<br>(Dohmann et al., 2005) |
| 26. | AJH1RV2 | TTCAAACATAAATGTGAAAAACAACAT | Genotyping *csn5a-2* plants<br>(Dohmann et al., 2005) |
| 27. | LBb1 | CAGCGTGGACCGCTTGCTGCAACTCTCTCA | T-DNA Left-border primer (for *csn5a-2*) |

| | | | |
|---|---|---|---|
| | | | (Dohmann et al., 2005) |
| 28. | *Bam*HI IPK1 For | CCGGATCCGAGATGATTTTGGAGGAG | Cloning IPK1 in *p*ET28a |
| 29. | *Sal*I IPK1 Rev | GGGTCGACTTAGCTGTGGGAAGGTTTTG | Cloning IPK1 in *p*ET28a |
| 30. | *Bam*HI ITPK1 For | GGGGATCCATGTCAGATTCAATCCA | Cloning ITPK1 in *p*GEX4T-3 |
| 31. | *Xho*I IPK1 Rev | GGCTCGAGTCAGACATGATTCTTCTT | Cloning ITPK1 in *p*GEX4T-3 |

987